

Total scattering / PDF: Theory and practice

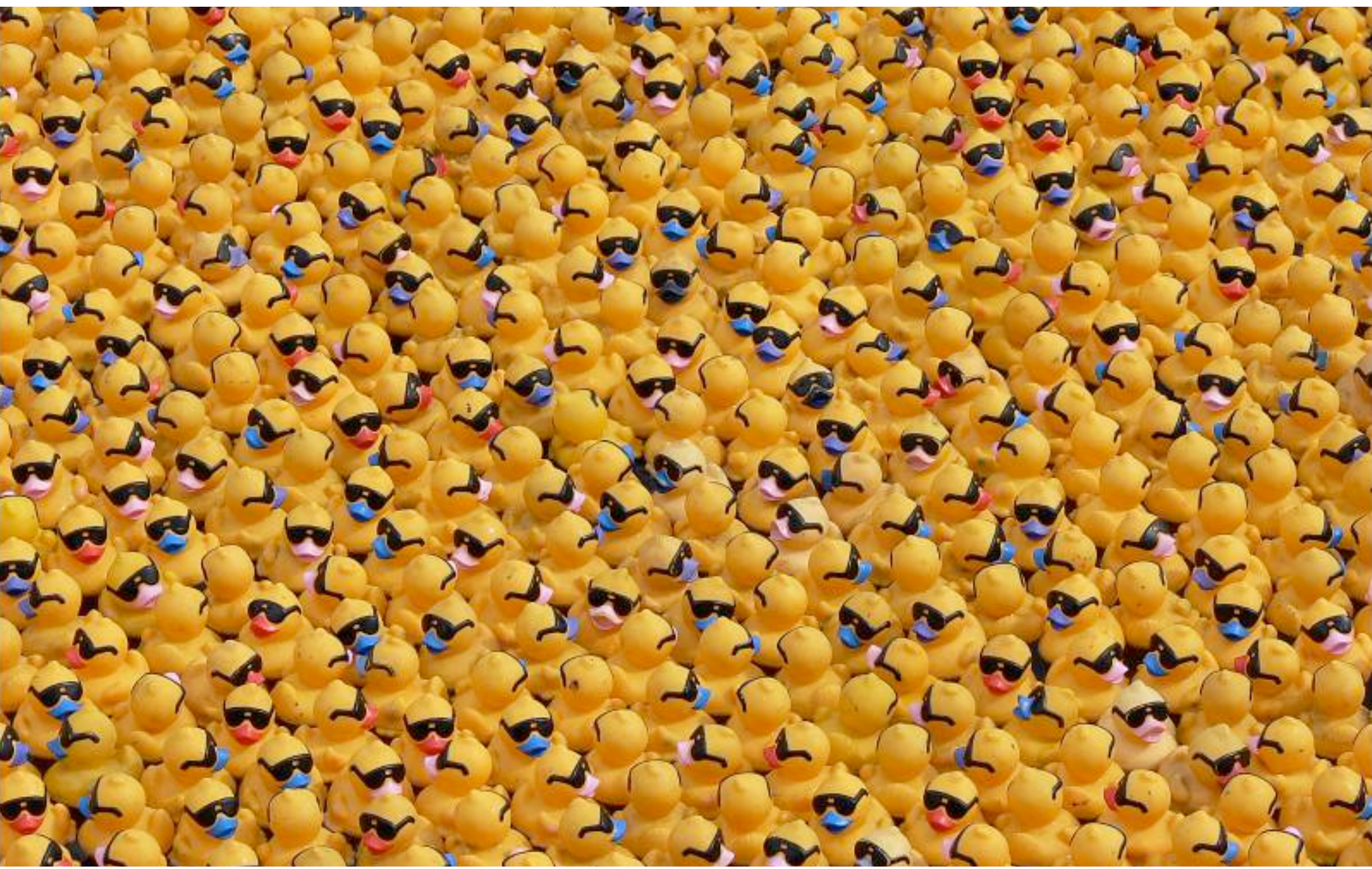
Andrew Goodwin
September 2017

Two ways of thinking about structure

Density of matter at a given point in space – $\rho(\mathbf{r})$

Amplitude of a density wave of given periodicity – $F(\mathbf{Q})$

Whereas the vectors \mathbf{r} lie in *real space* (units Å),
the wave vectors \mathbf{Q} lie in *reciprocal space* (units Å⁻¹)

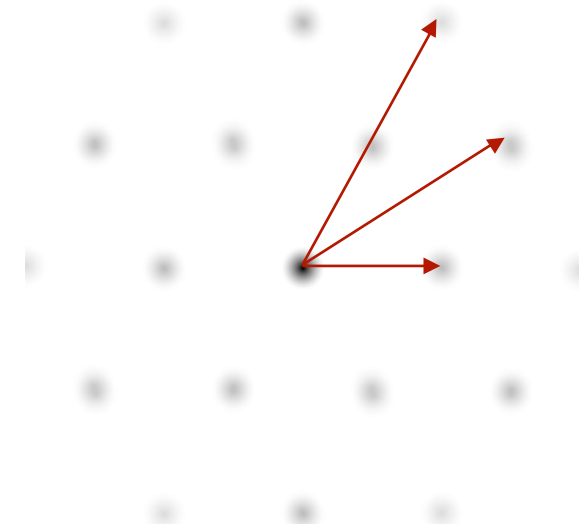
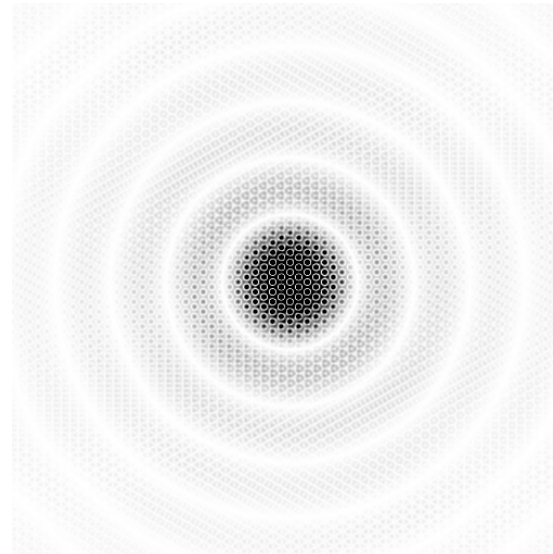
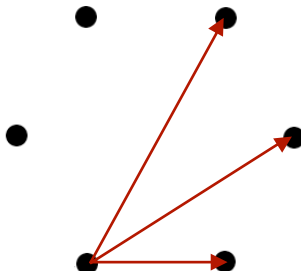


$$\begin{aligned}F(\mathbf{Q}) &= \int \rho(\mathbf{r}) \exp(i\mathbf{Q} \cdot \mathbf{r}) d\mathbf{r}, \\ \rho(\mathbf{r}) &= \frac{1}{2\pi} \int F(\mathbf{Q}) \exp(-i\mathbf{Q} \cdot \mathbf{r}) d\mathbf{Q}.\end{aligned}$$

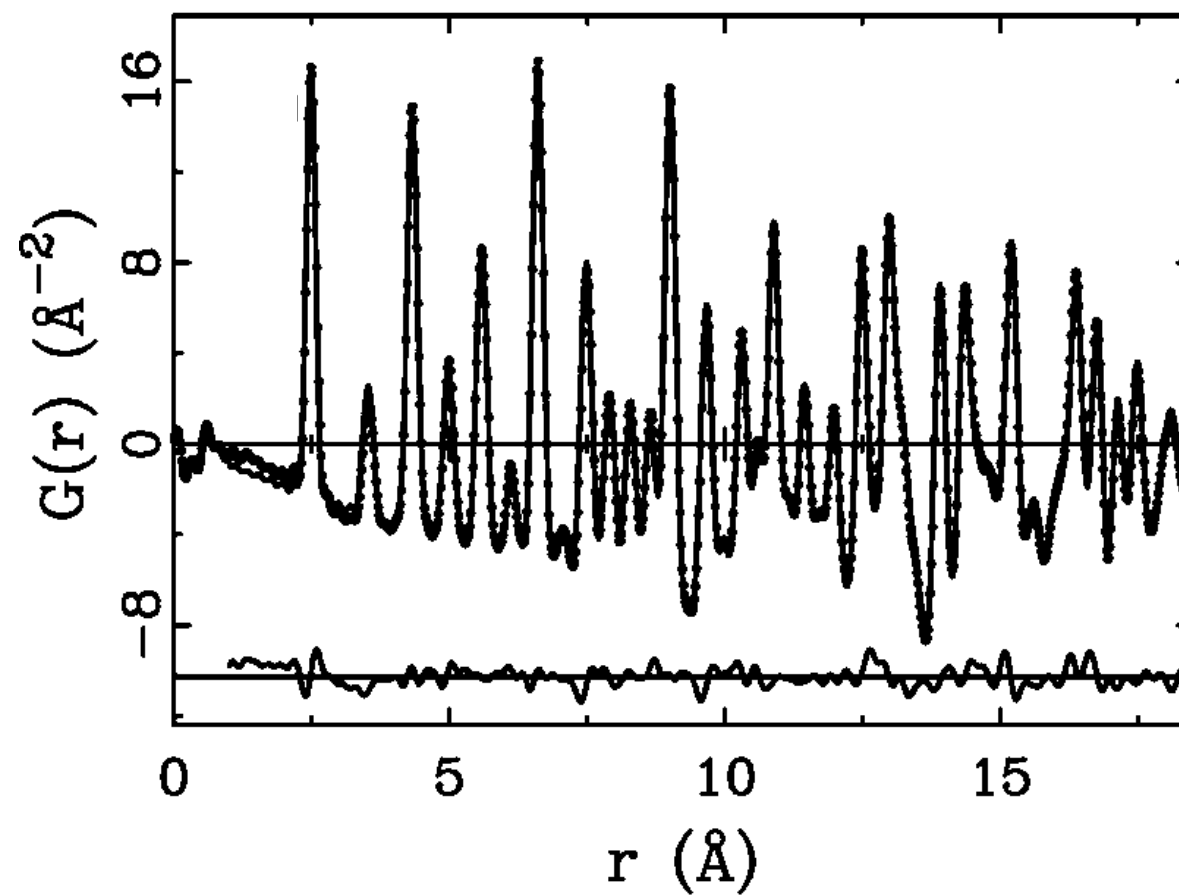
$$\begin{aligned}
I(\mathbf{Q}) \propto |F(\mathbf{Q})|^2 &= \left| \int \rho(\mathbf{r}) \exp(i\mathbf{Q} \cdot \mathbf{r}) d\mathbf{r} \right|^2 \\
&= \int \rho(\mathbf{r}) \exp(i\mathbf{Q} \cdot \mathbf{r}) d\mathbf{r} \times \int \rho(\mathbf{r}) \exp(-i\mathbf{Q} \cdot \mathbf{r}) d\mathbf{r} \\
&= \iint \rho(\mathbf{r}_j - \mathbf{r}_i) \exp[i\mathbf{Q} \cdot (\mathbf{r}_j - \mathbf{r}_i)] d\mathbf{r}_i d\mathbf{r}_j.
\end{aligned}$$

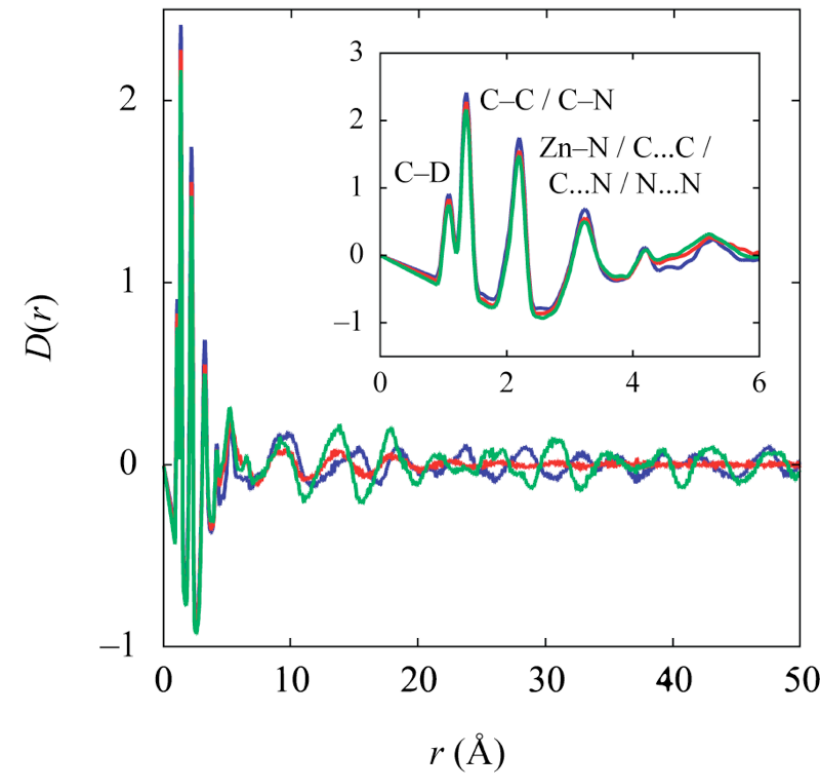
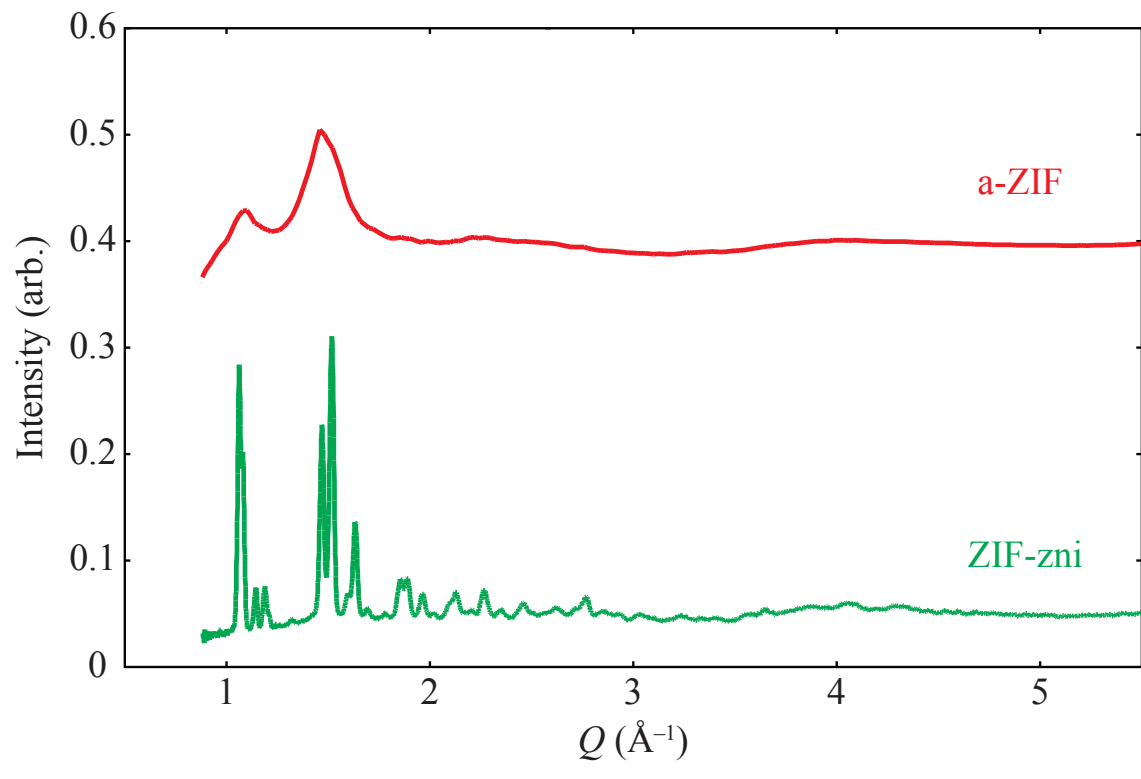
Patterson function

Fourier transform of intensities
tells us about pair distribution function $\rho(\mathbf{r}_j - \mathbf{r}_i)$



1D: pair distribution function





Received 31 July 2000

Accepted 8 December 2000

A comparison of various commonly used correlation functions for describing total scattering

David A. Keen

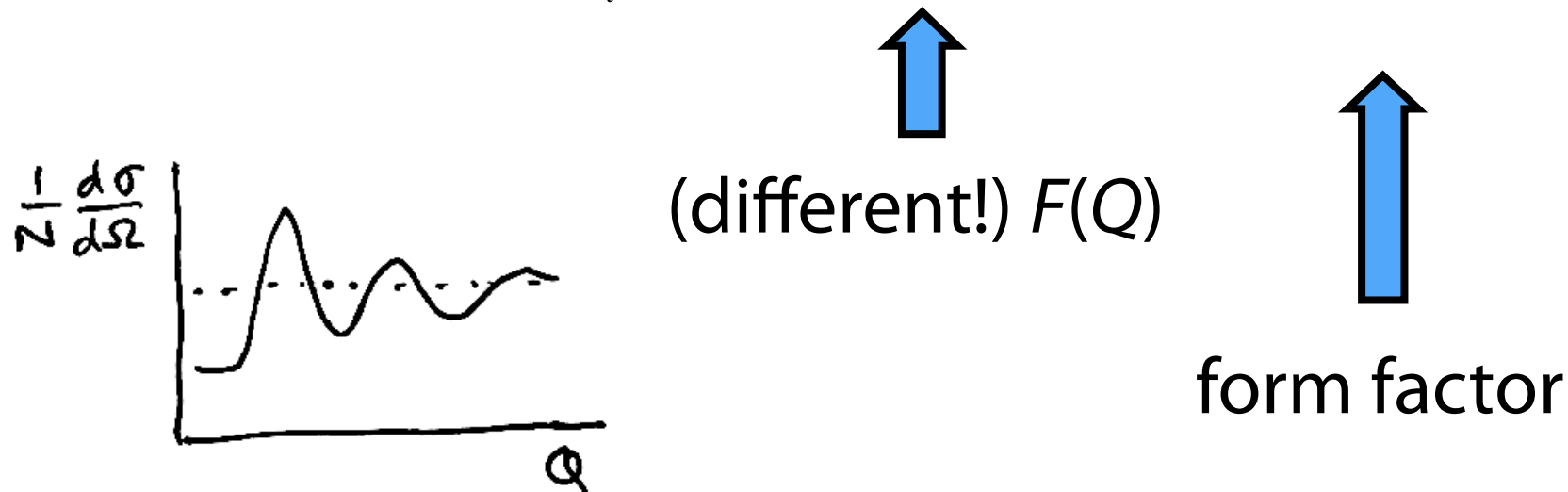
ISIS Facility, Rutherford Appleton Laboratory, Chilton, Didcot, Oxfordshire OX11 0QX, England.
Correspondence e-mail: d.a.keen@rl.ac.uk

Total scattering, an increasingly important crystallographic research area, is defined theoretically in terms of correlation functions. Different researchers use different definitions for these functions, frequently leading to confusion in the literature. Here, a consistent set of equations for total-scattering correlation functions are developed and explicitly compared with other, often encountered, definitions. It is hoped that this will lead to increased transparency for newcomers to the field of total scattering.

© 2001 International Union of Crystallography
Printed in Great Britain – all rights reserved

Normalised scattering cross section

$$\frac{1}{N} \frac{d\sigma}{d\Omega} = \sum_{i,j=1}^n c_i c_j \bar{b}_i \bar{b}_j [A_{ij}(Q) - 1] + \sum_{i=1}^n c_i \bar{b}_i^2. \quad (5)$$

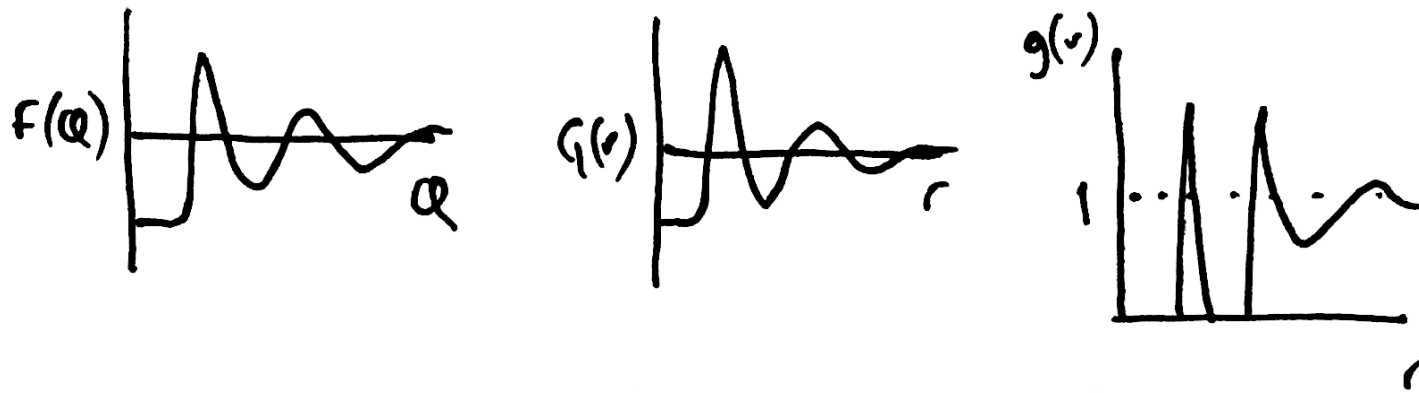


$$\frac{1}{N} \frac{d\sigma}{d\Omega} = \sum_{i,j=1}^{\infty} c_i c_j b_i b_j \left[A_{ij}(Q) - 1 \right] + \sum_{i=1}^n c_i \bar{b}_i^2. \quad (11)$$

$$G(r) = \frac{1}{(2\pi)^3 \rho_0} \int_0^\infty 4\pi Q^2 F(Q) \frac{\sin Qr}{Qr} = \sum_{i,j=1}^n c_i c_j \bar{b}_i \bar{b}_j [g_{ij}(r) - 1] \quad (10) \quad (12)$$

$$g_{ij}(r) = \frac{n_{ij}(r)}{4\pi r^2 dr \rho_j}, \quad (8)$$

where $n_{ij}(r)$ are the number of particles of type j between distances r and $r + dr$ from a particle of type i and $\rho_j = c_j \rho_0$.



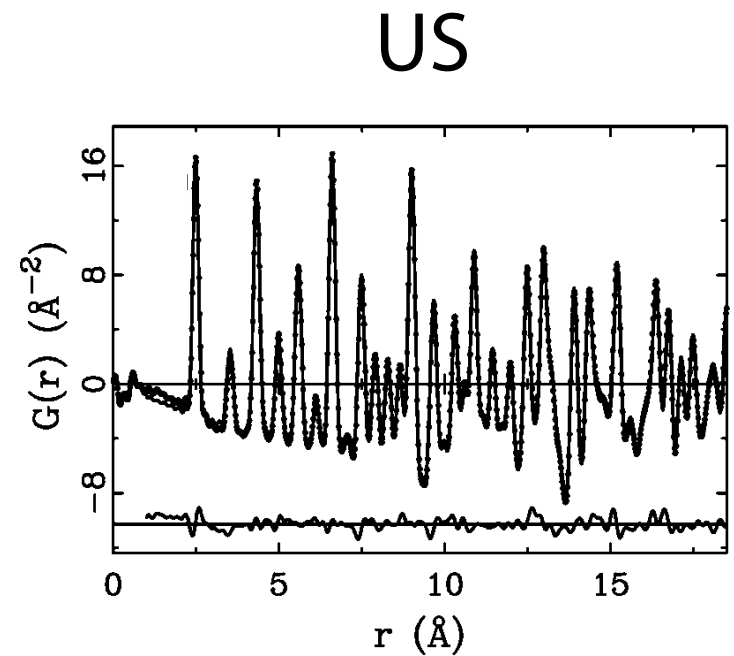
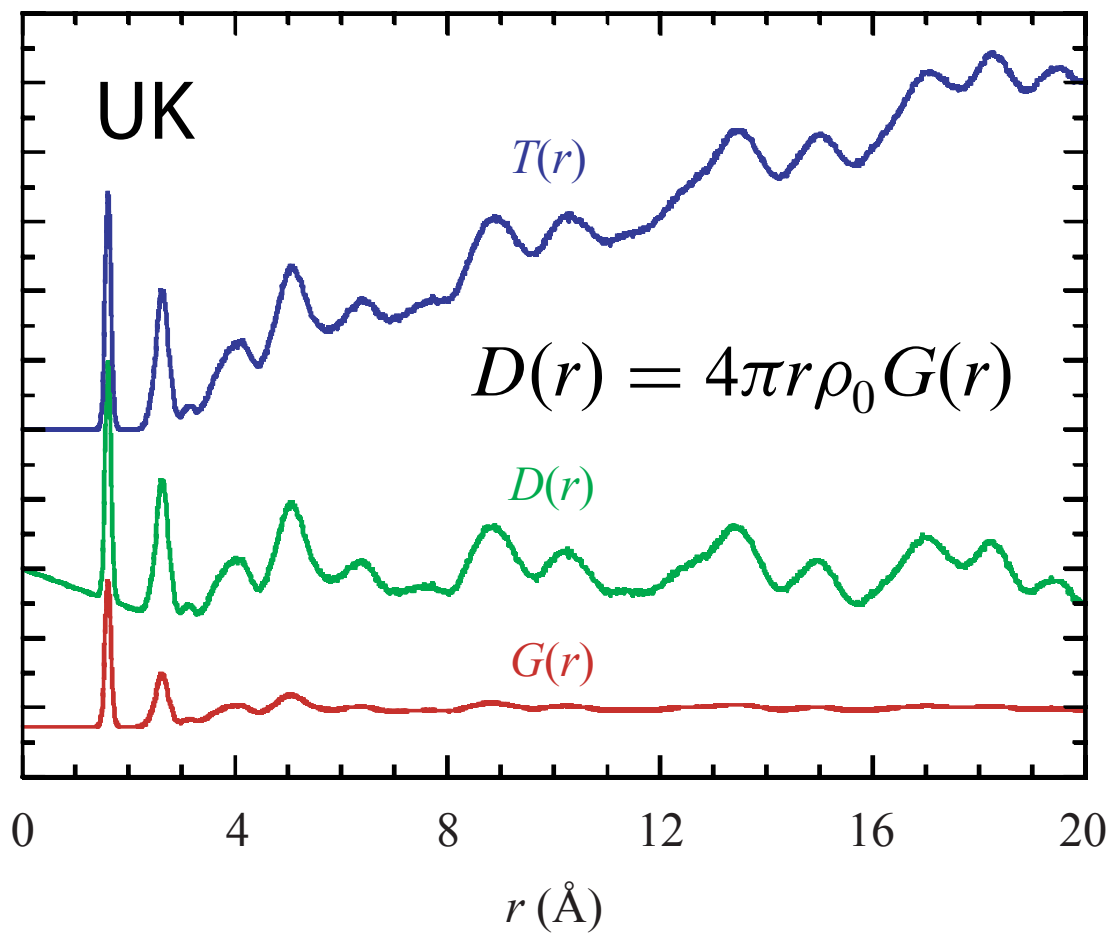
$$F(Q) = \rho_0 \int_0^\infty 4\pi r^2 G(r) \frac{\sin Qr}{Qr} dr \quad (11)$$

$$G(r) = \frac{1}{(2\pi)^3 \rho_0} \int_0^\infty 4\pi Q^2 F(Q) \frac{\sin Qr}{Qr} = \sum_{i,j=1}^n c_i c_j \bar{b}_i \bar{b}_j [g_{ij}(r) - 1] \quad (10) \quad (12)$$

$$g_{ij}(r) = \frac{n_{ij}(r)}{4\pi r^2 dr \rho_j}, \quad (8)$$

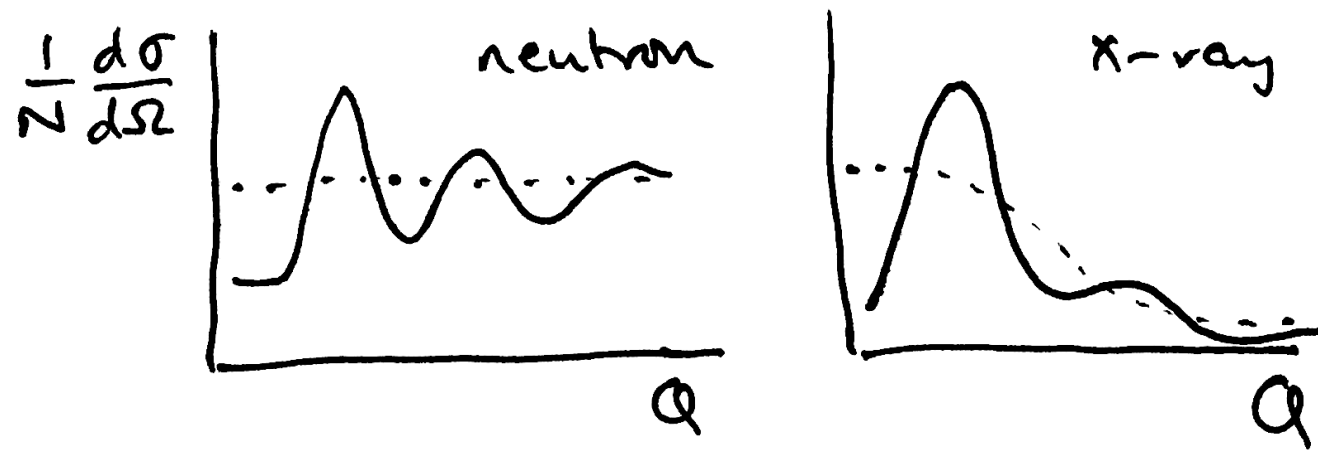
where $n_{ij}(r)$ are the number of particles of type j between distances r and $r + dr$ from a particle of type i and $\rho_j = c_j \rho_0$.

Alternative normalisations



$$D(r) = G^{\text{PDF}}(r) \left(\sum_{i=1}^n c_i b_i \right)^2$$

X-ray PDF

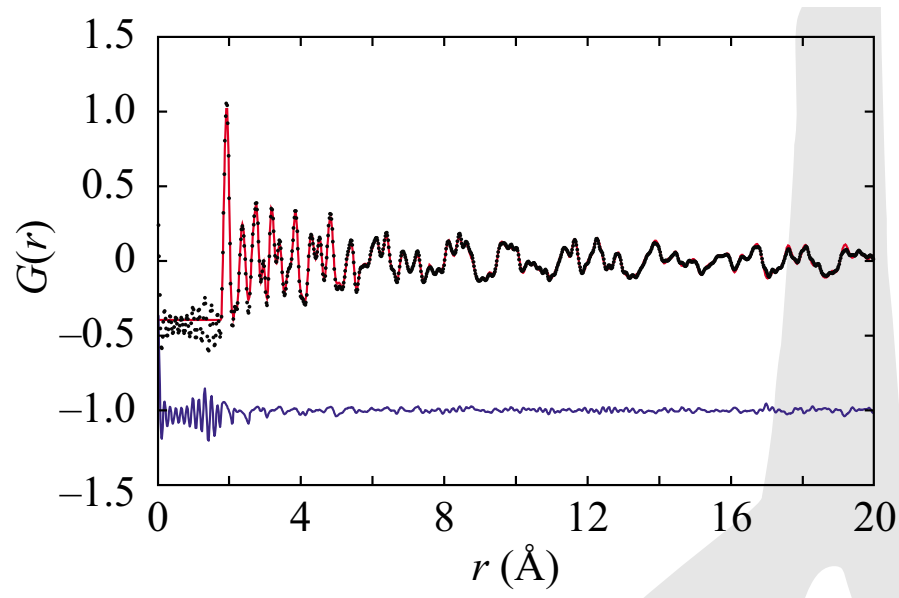


$$F^X(Q) = \left[\frac{1}{N} \frac{d\sigma}{d\Omega} - \sum_{i=1}^n c_i f_i(Q)^2 \right] / \left[\sum_{i=1}^n c_i f_i(Q) \right]^2. \quad (55)$$

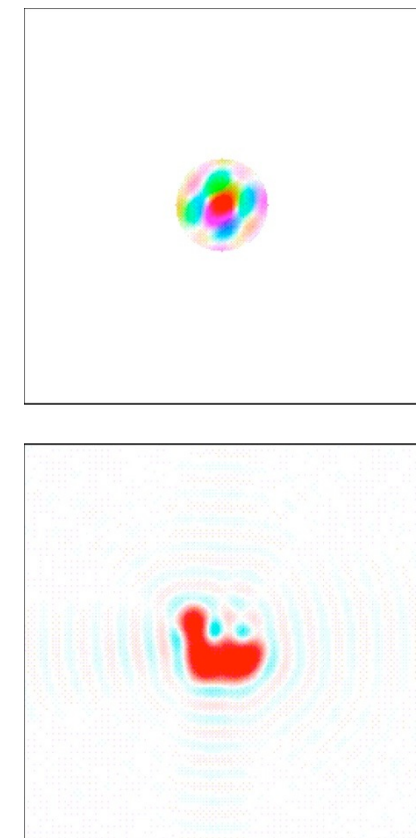
$$G^X(r) = \frac{1}{(2\pi)^3 \rho_0} \int_0^\infty 4\pi Q^2 F^X(Q) \frac{\sin Qr}{Qr} dQ, \quad (58)$$

Termination ripples

$$G(r) = \frac{1}{(2\pi)^3 \rho_0} \int_0^\infty 4\pi Q^2 F(Q) \frac{\sin Qr}{Qr} dQ$$



$$\Delta r \simeq \frac{3.791}{Q_{\max}}$$



Experimental constraints

Low and understandable background

Large Q_{\max} (typically 20 \AA^{-1} ; preferably 40 \AA^{-1})

Hence spallation neutron sources and
high-energy X-rays (synchrotrons / Ag)

$$Q = \frac{4\pi}{\lambda} \sin \theta$$

Data normalisation

Dark Arts: work with instrument scientists!

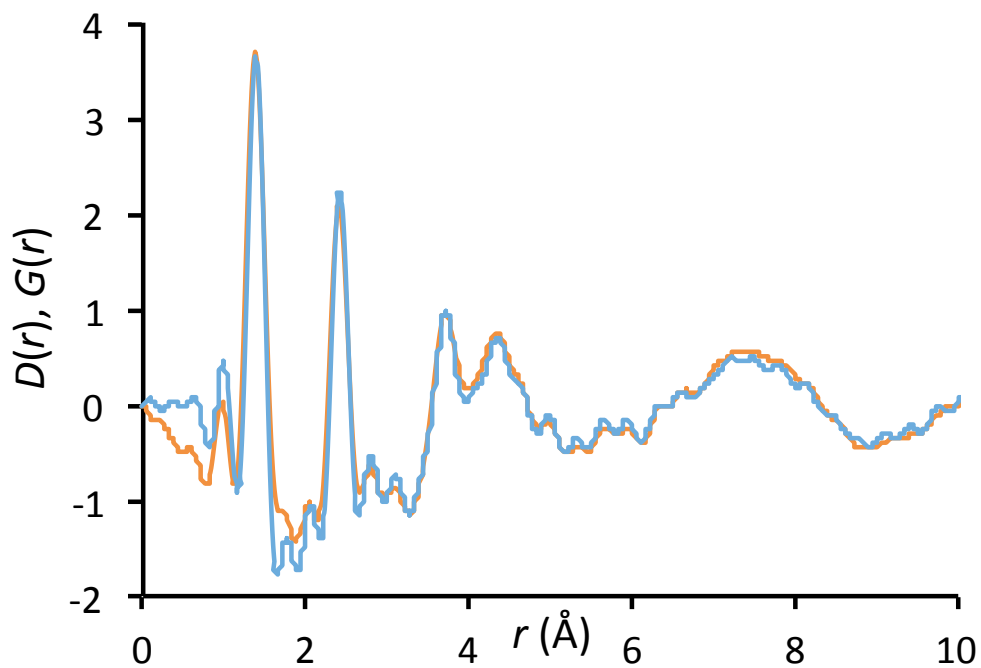
GUDRUN / GUDRUNX

PDFGETN / PDFGETX(3)

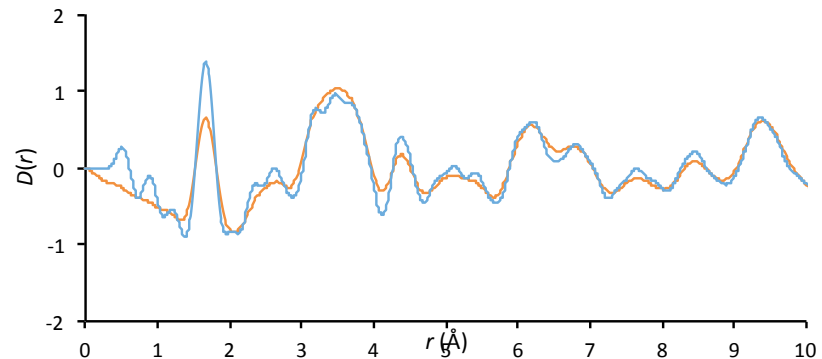
Accounts for background, multiple scattering,
absorption, fluorescence, inelasticity,...

GUDRUNX vs PDFGETX3

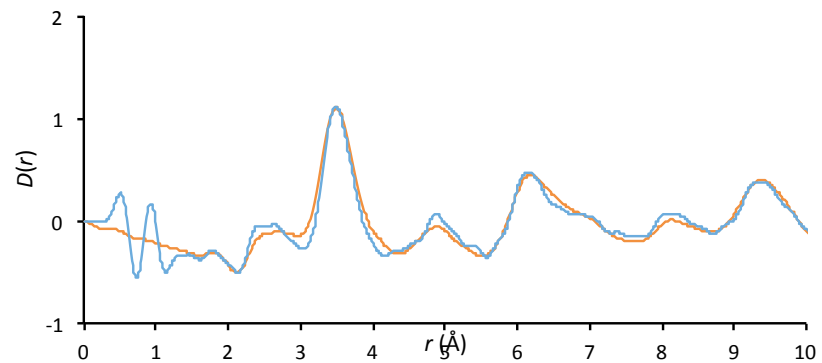
CBZ

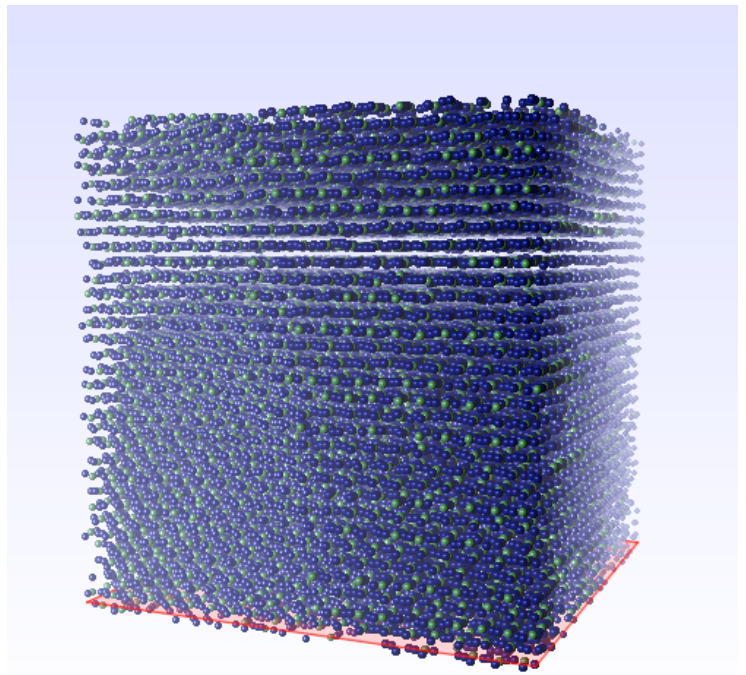
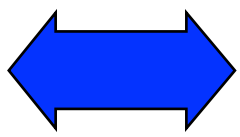
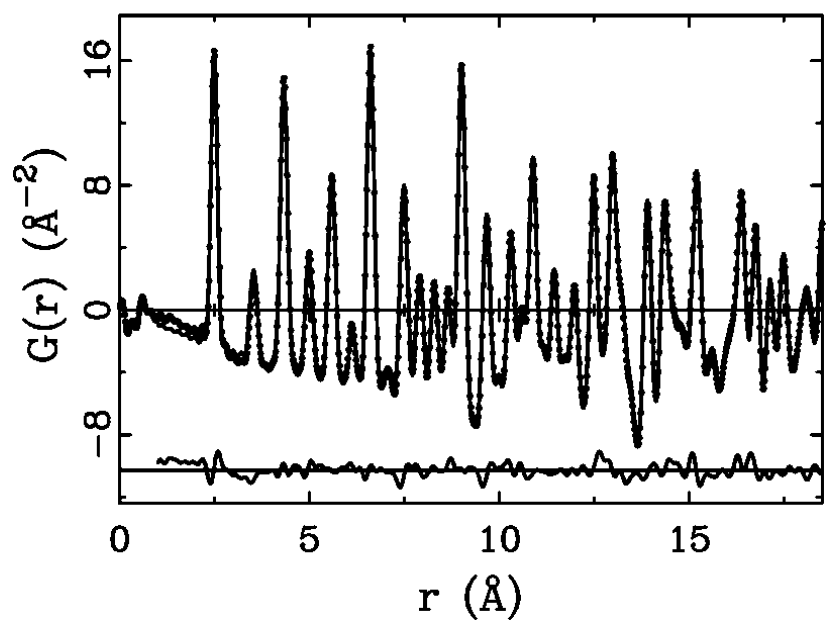


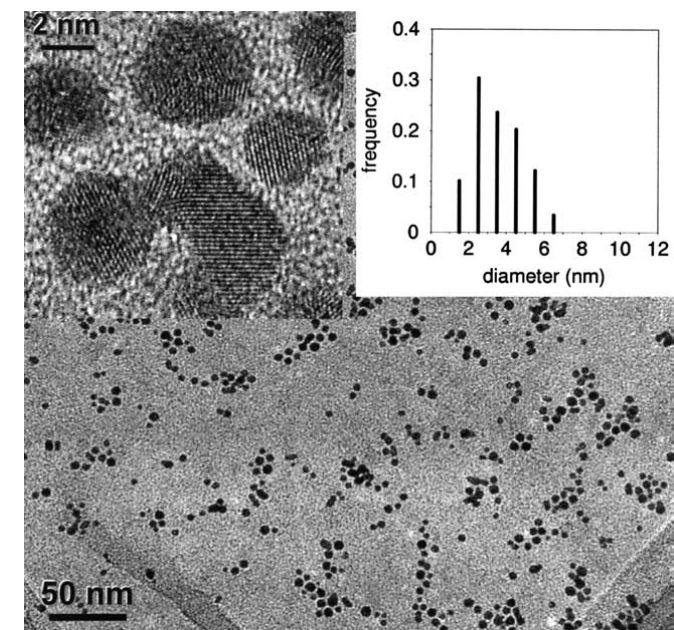
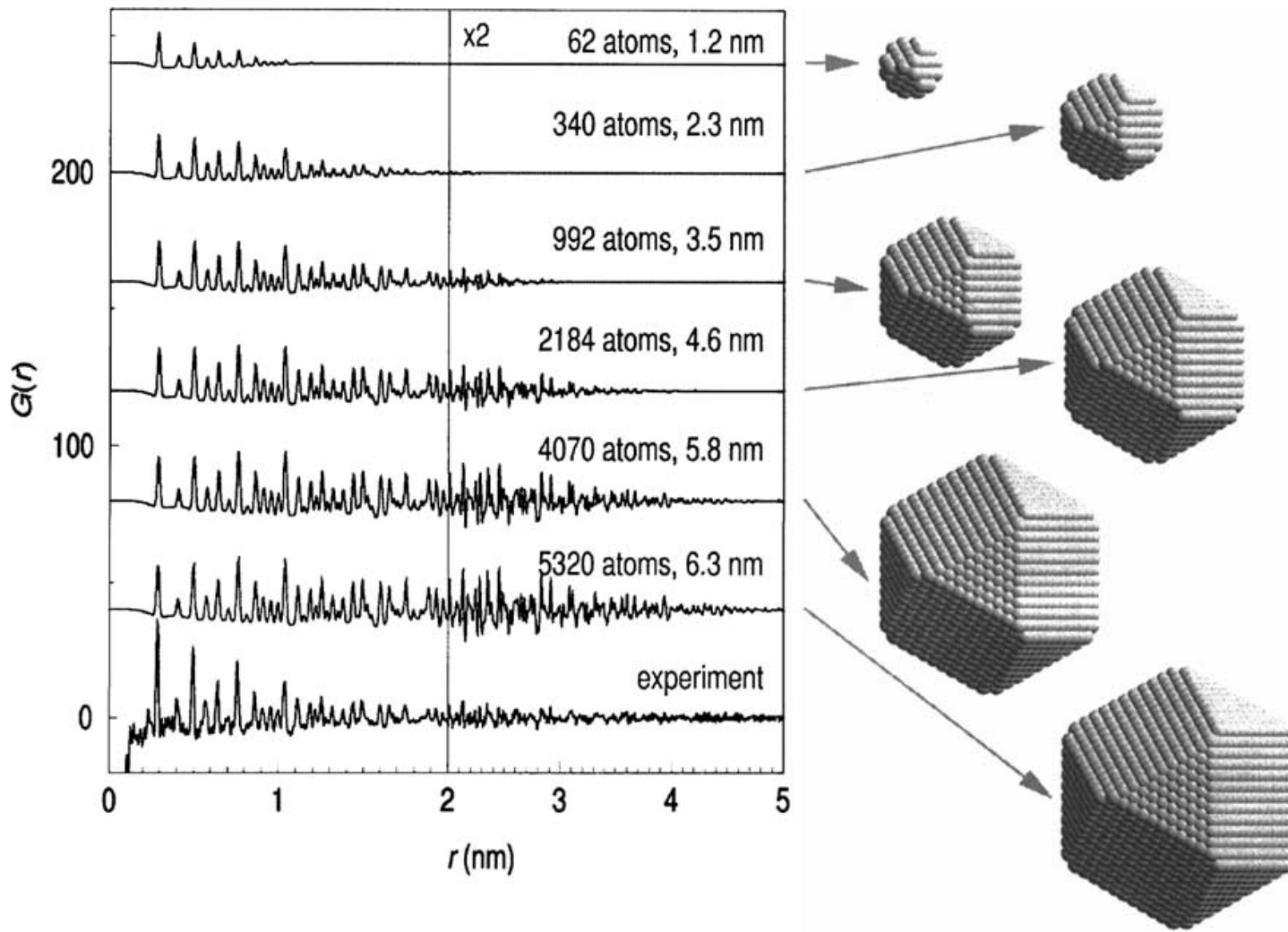
FAUX

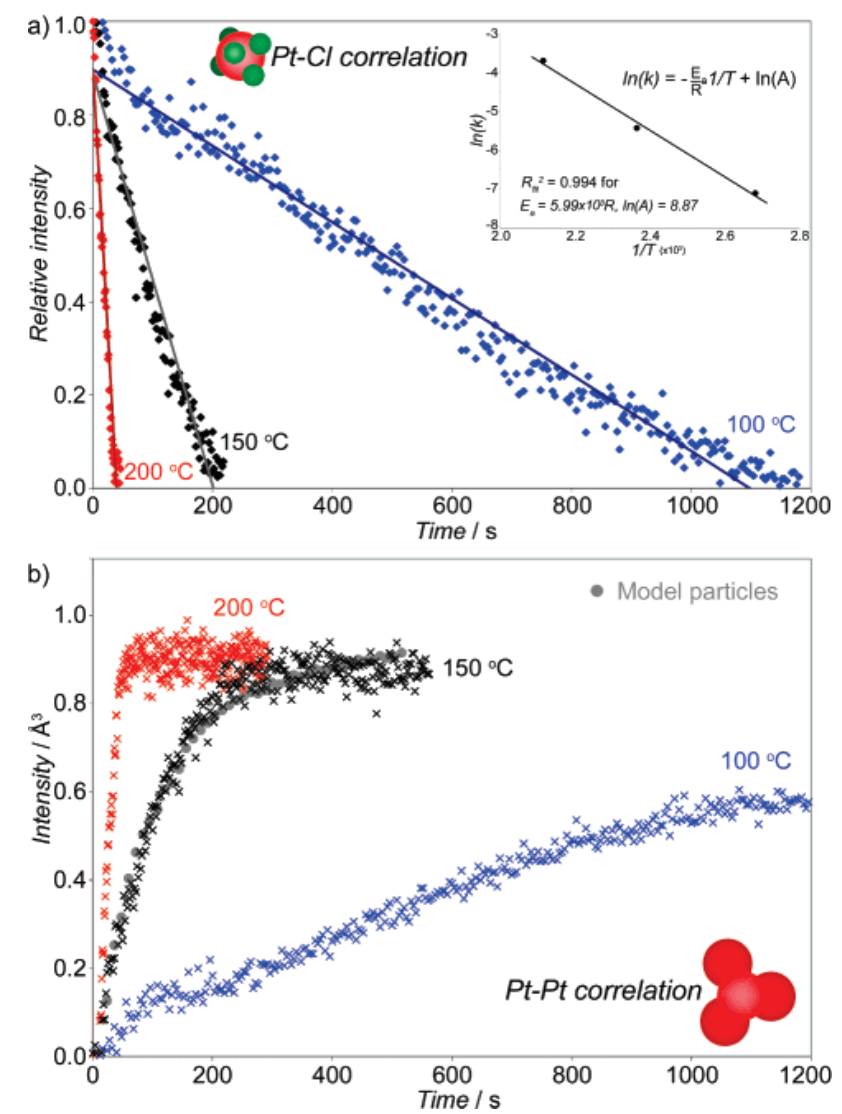
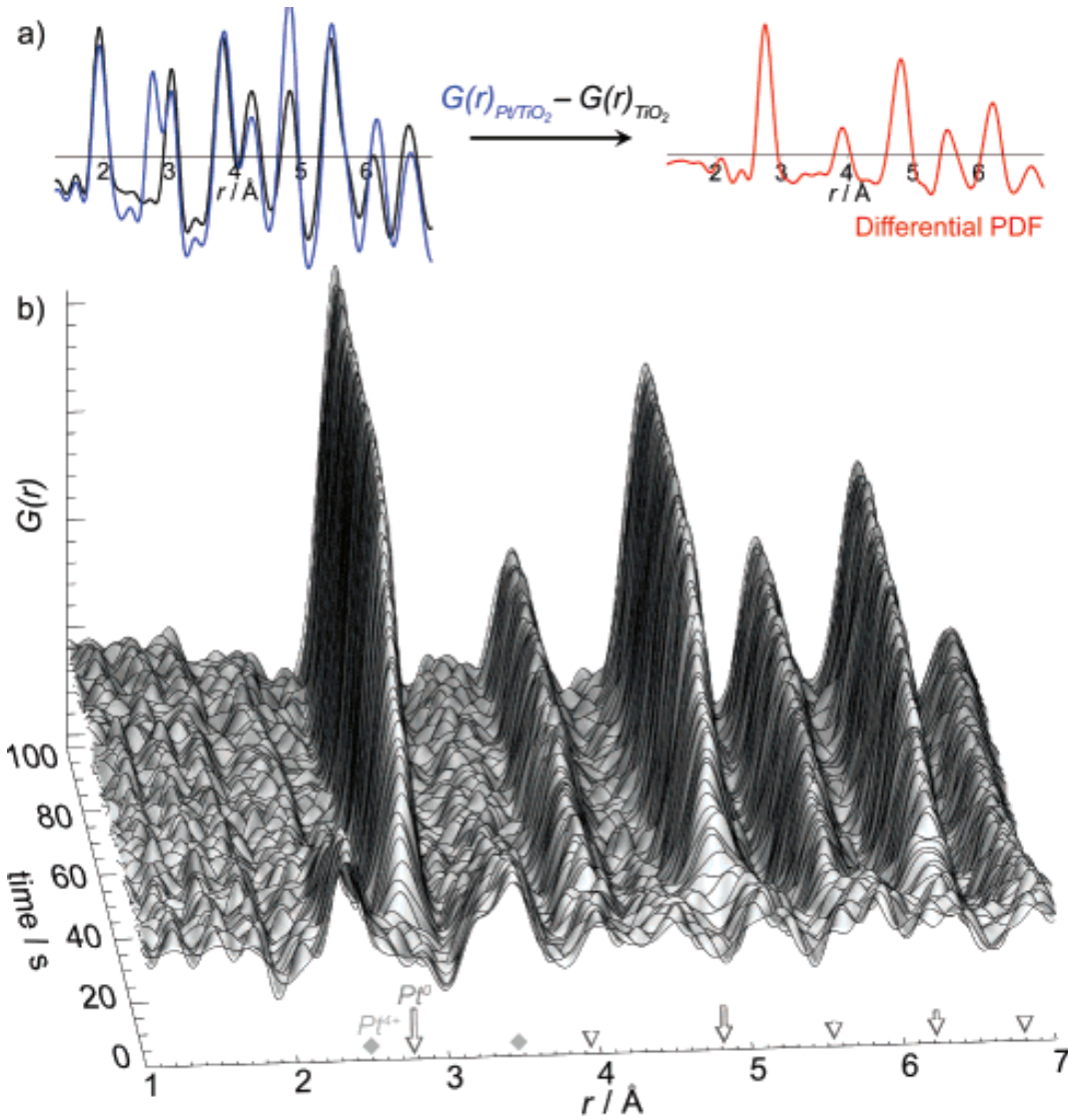


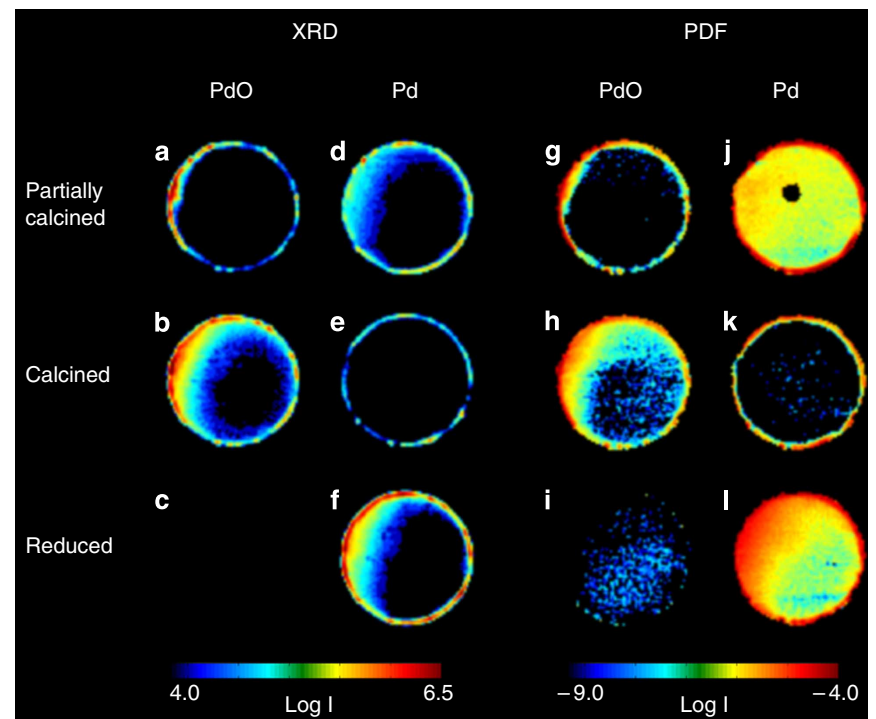
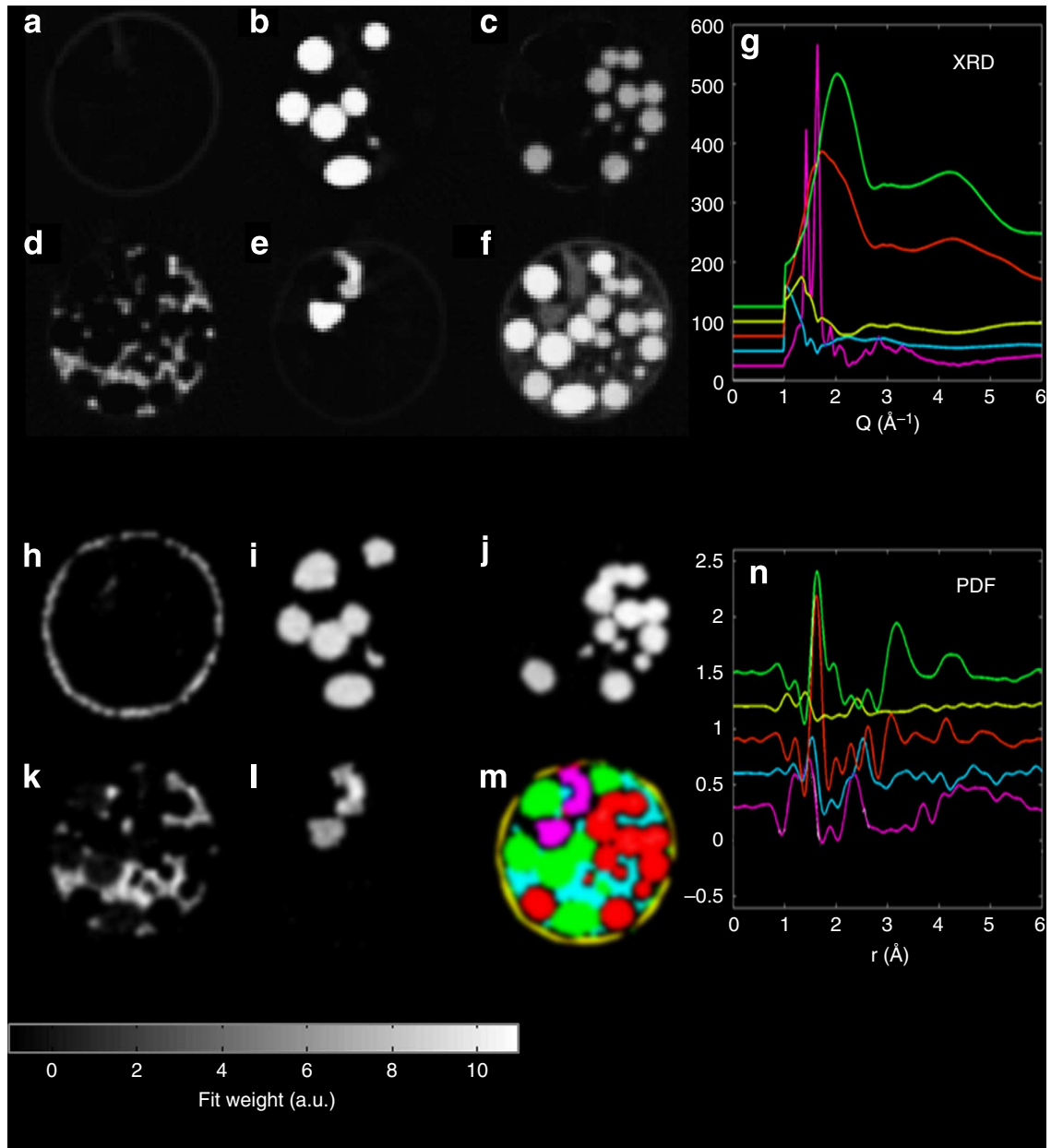
FAUX











Fitting the PDF

Small box

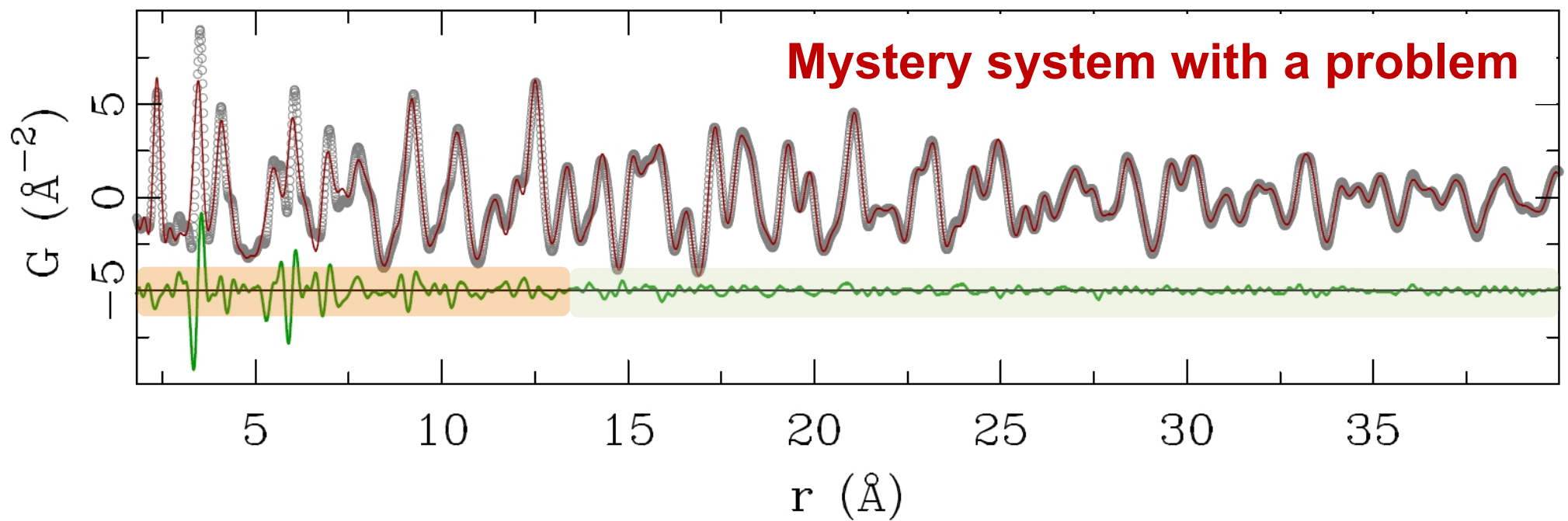
“Real-space Rietveld”
(PDFfit / PDFGui)

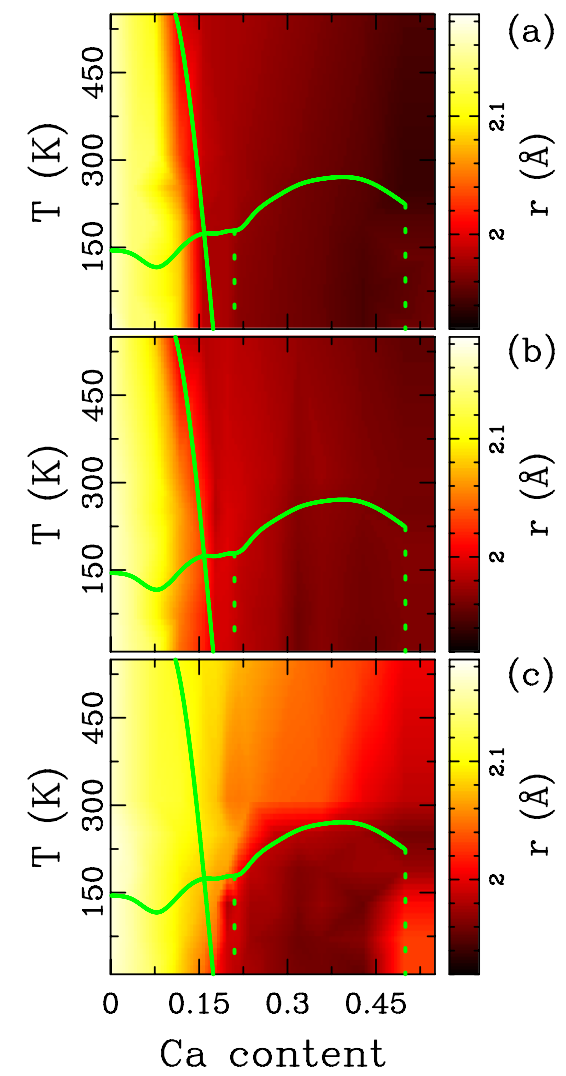
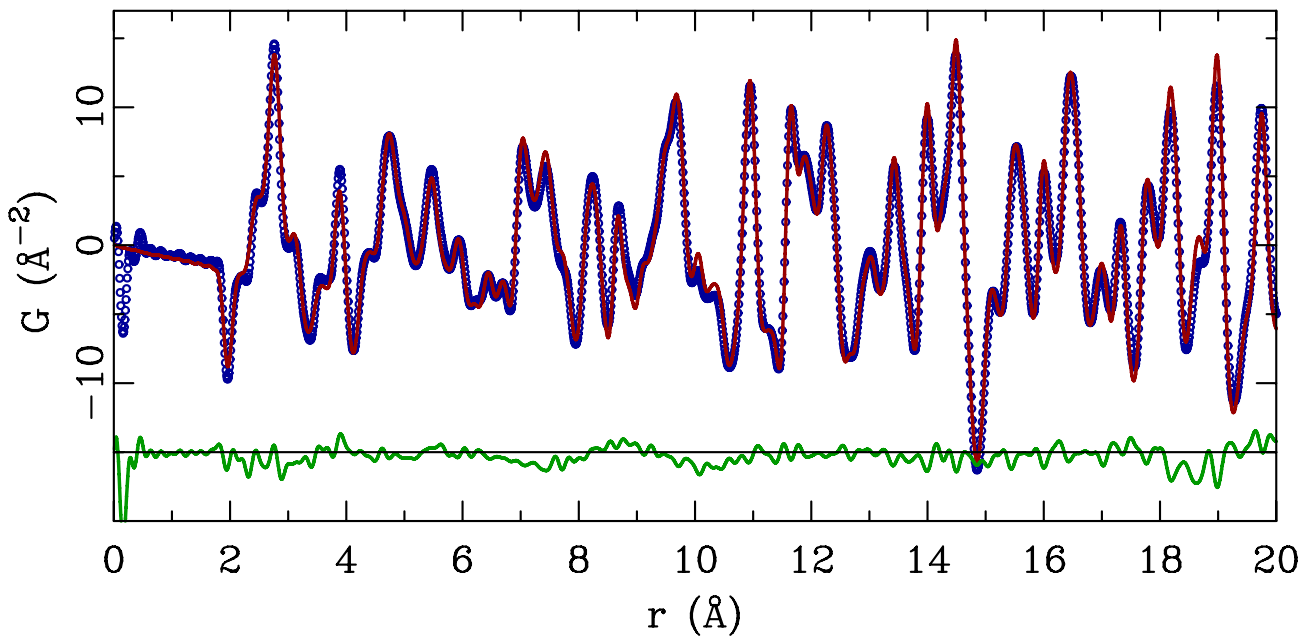
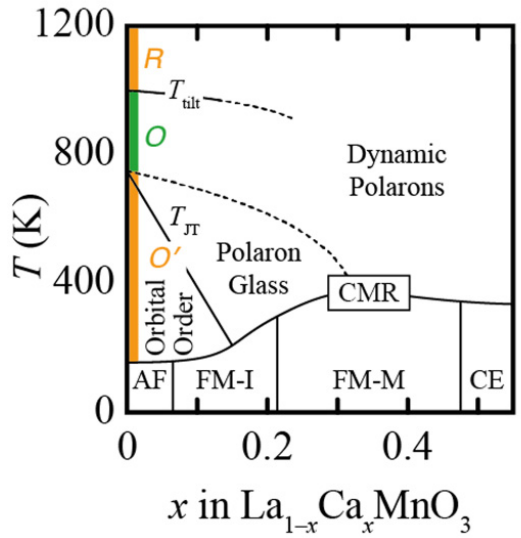
Big box

Reverse Monte Carlo
(RMCProfile)

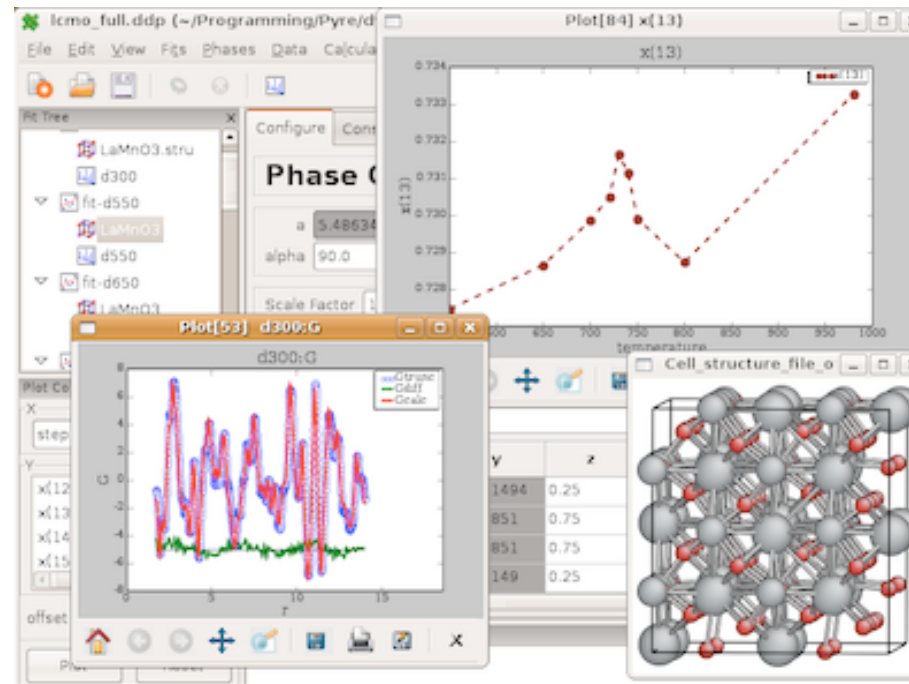
Empirical Potential
Structure Refinement
(EPSR)

Small box science





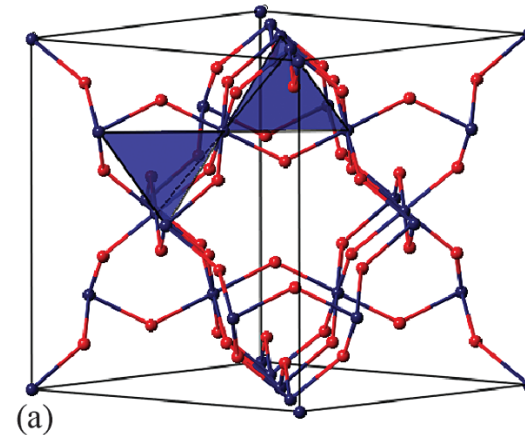
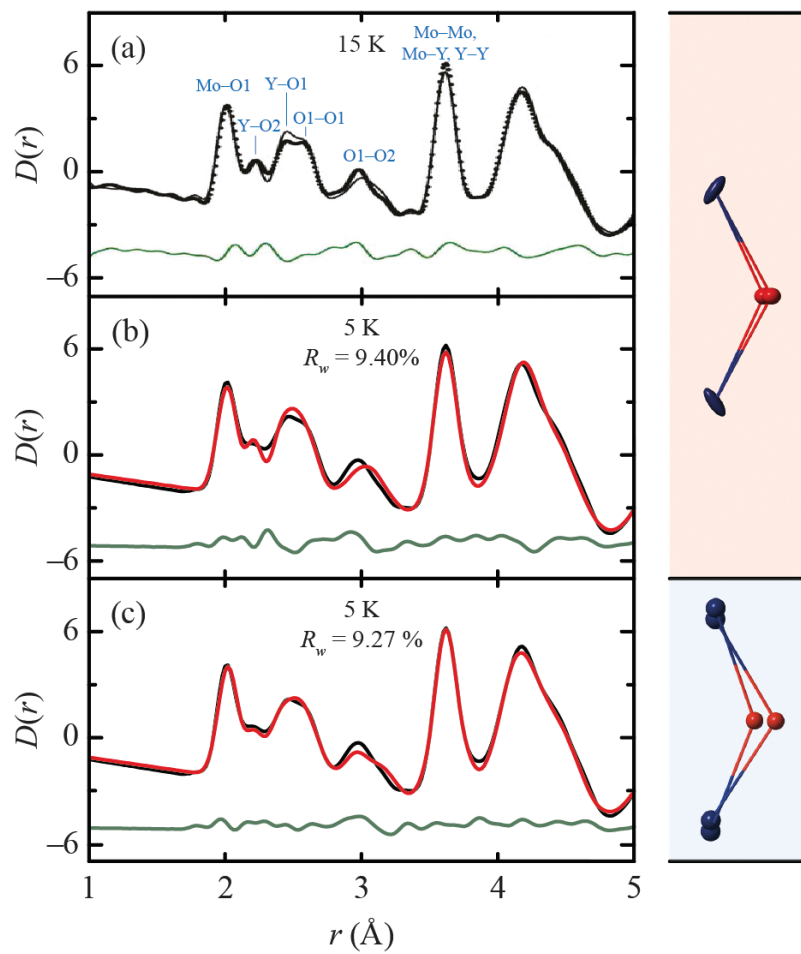
PDFGui



$$G_{calc}(r) = \frac{1}{Nr\langle b \rangle^2} \sum_{i \neq j} b_i b_j \frac{1}{\sqrt{2\pi}\sigma_{ij}} \exp \left[-\frac{(r - r_{ij})^2}{2\sigma_{ij}^2} \right] - 4\pi r \rho_0$$

$$B(r) = e^{-\frac{(rQ_{damp})^2}{2}}$$
$$\sigma_{ij} = \sigma'_{ij} \sqrt{1 - \frac{\delta_1}{r_{ij}} - \frac{\delta_2}{r_{ij}^2} + Q_{broad}^2 r_{ij}^2}$$

PDFGui



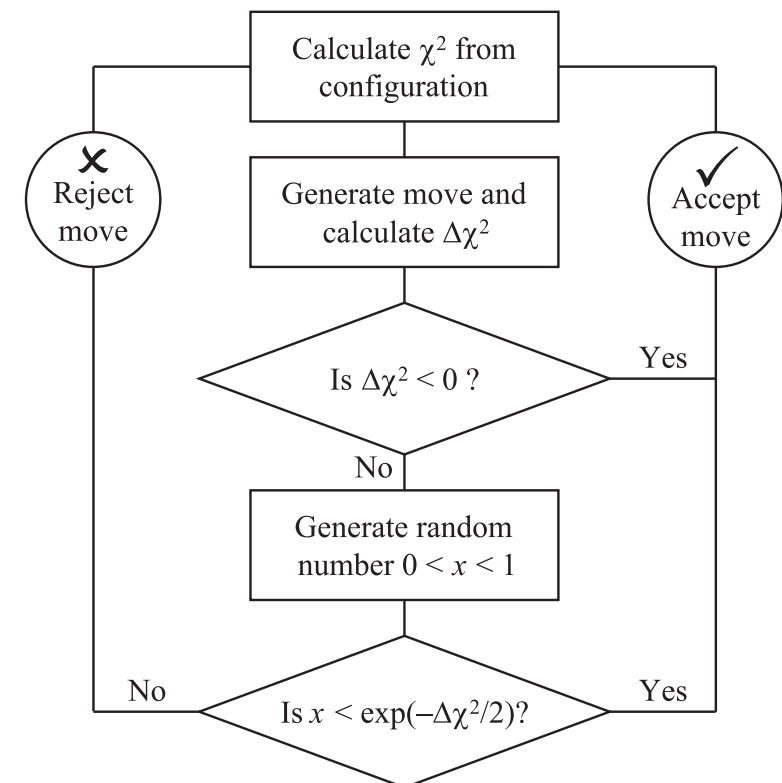
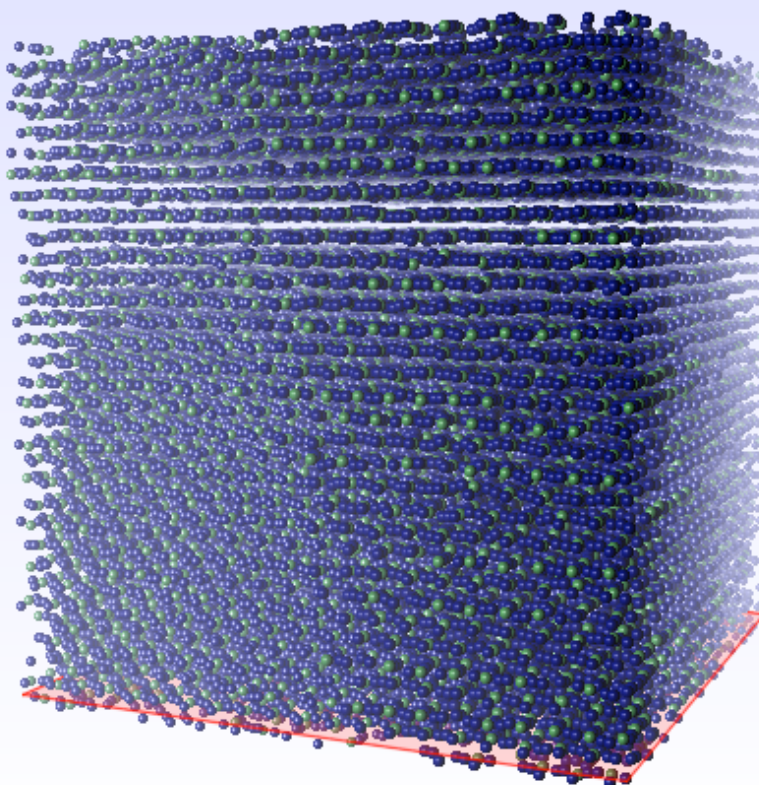
	<i>Split-site model</i> [29]	<i>Orbital dimer model</i>
a	10.2255(10)	$c_t \equiv \sqrt{2}a_t$ 10.2269(10)
$x(\text{O1a})$	0.3320(6)	$y(\text{Mo})$ 0.7371(8)
$x(\text{O1b})$	0.3446(6)	$z(\text{O1a})$ 0.6938(6)
$U_{11}(\text{Y})$	0.512(15)	$x(\text{O1b})$ 0.7184(5)
$U_{12}(\text{Y})$	-0.129(19)	$y(\text{O1b})$ 0.7910(5)
$U_{11}(\text{Mo})$	1.39(5)	$z(\text{O1b})$ 0.2467(4)
$U_{12}(\text{Mo})$	0.93(5)	$z(\text{O1c})$ 0.2709(6)
$U_{11}(\text{O1})$	1.02(11)	$U_{\text{iso}}(\text{Y})$ 0.355(11)
$U_{22}(\text{O1})$	0.81(3)	$U_{\text{iso}}(\text{Mo})$ 1.14(5)
$U_{\text{iso}}(\text{O2})$	0.55(3)	$U_{\text{iso}}(\text{O})$ 0.89(2)

Small box: pros and cons

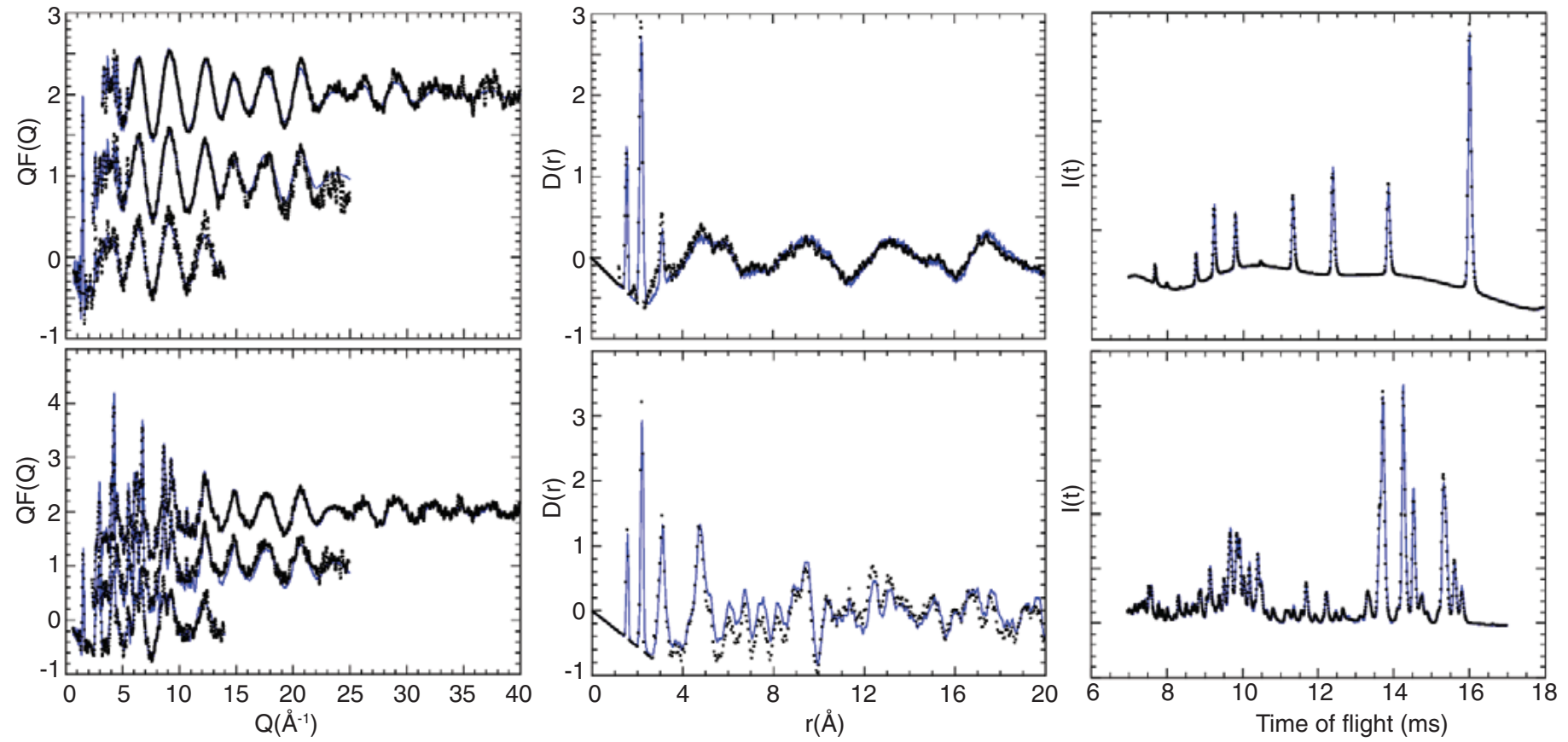
- + Very quick
- + Low entry barrier
- + Domain sizes / nanoparticles straightforward

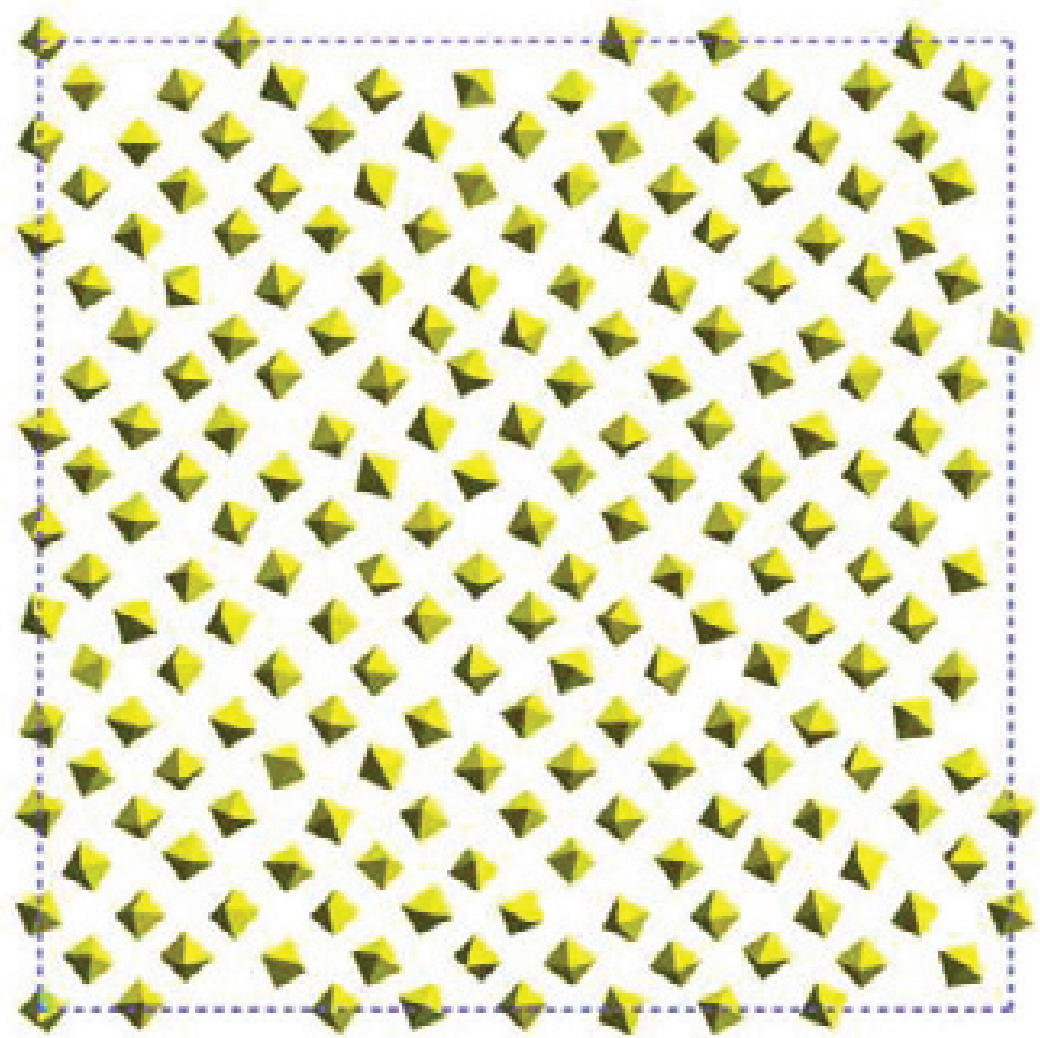
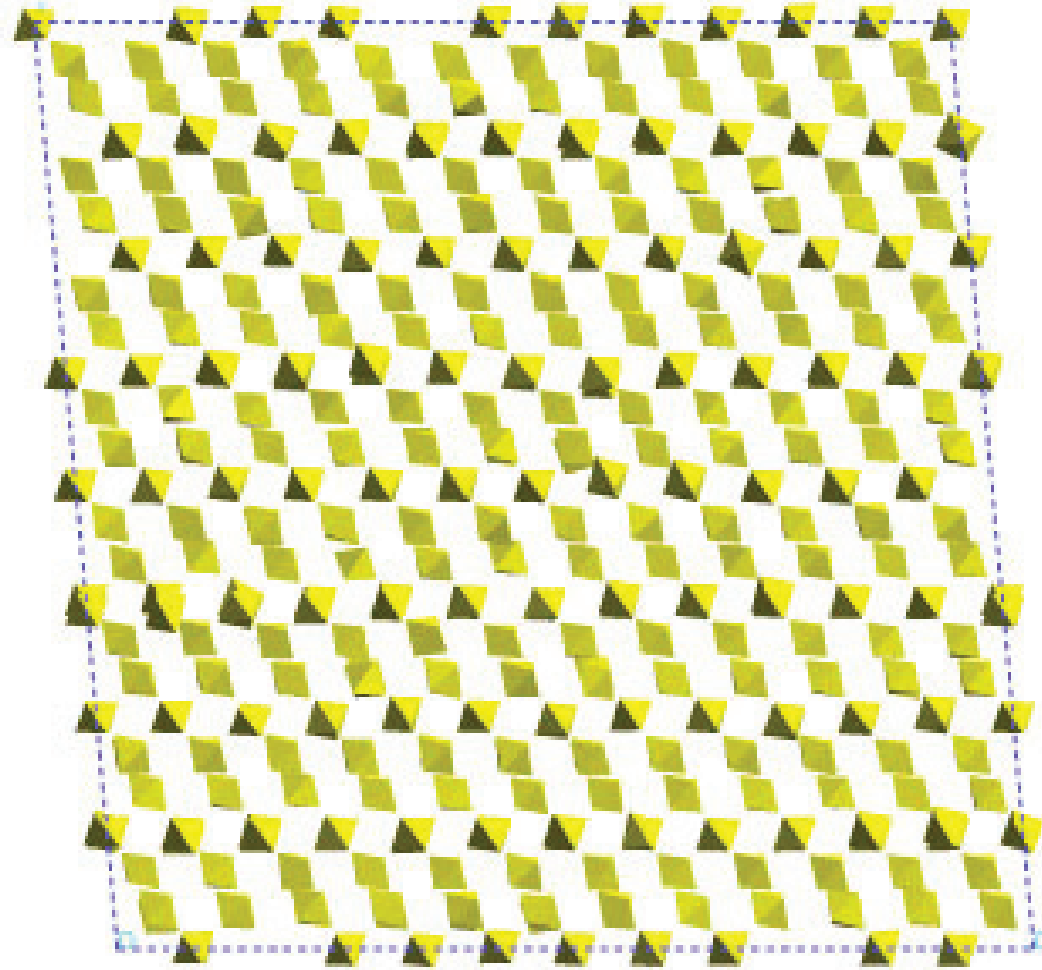
- Need starting model
- Need periodicity
- Is there a better model?

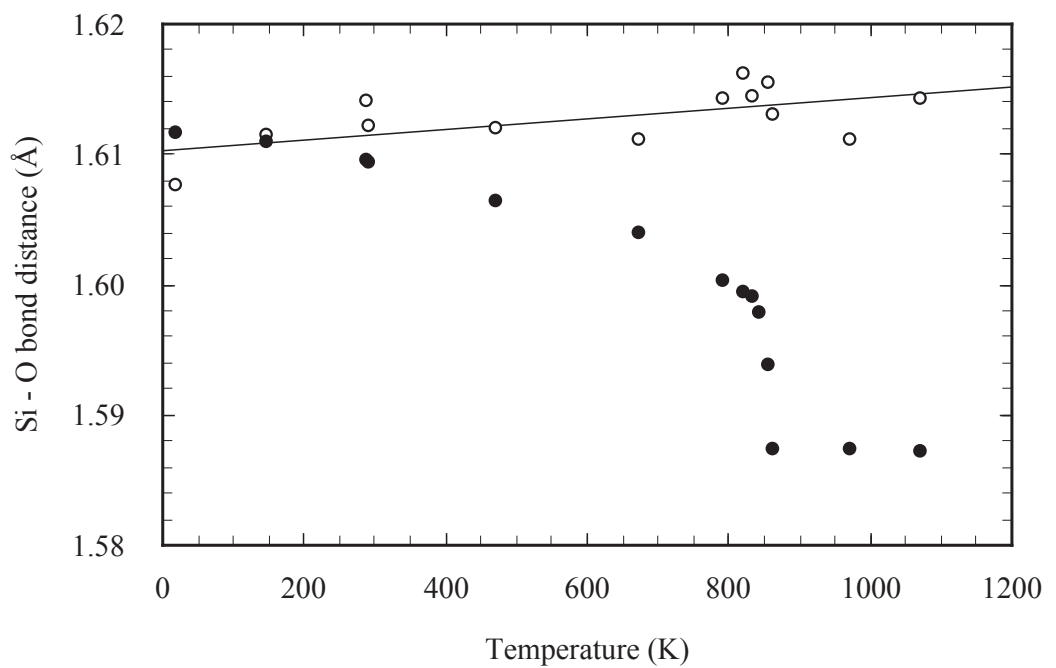
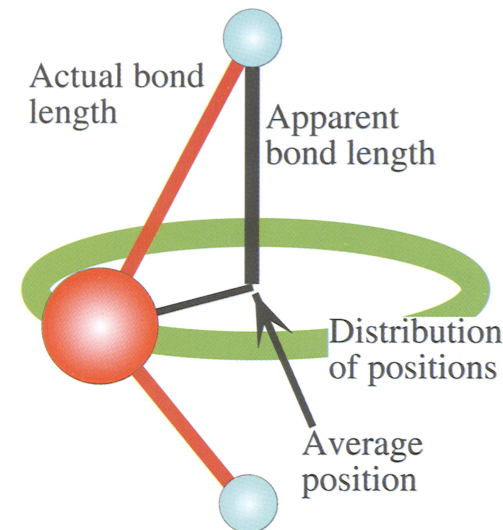
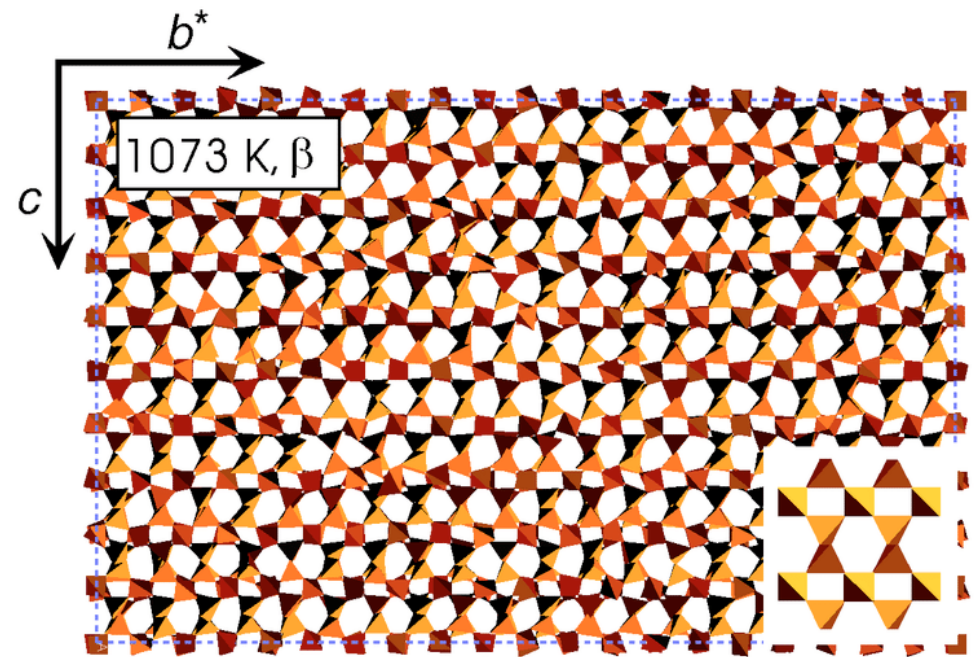
RMC

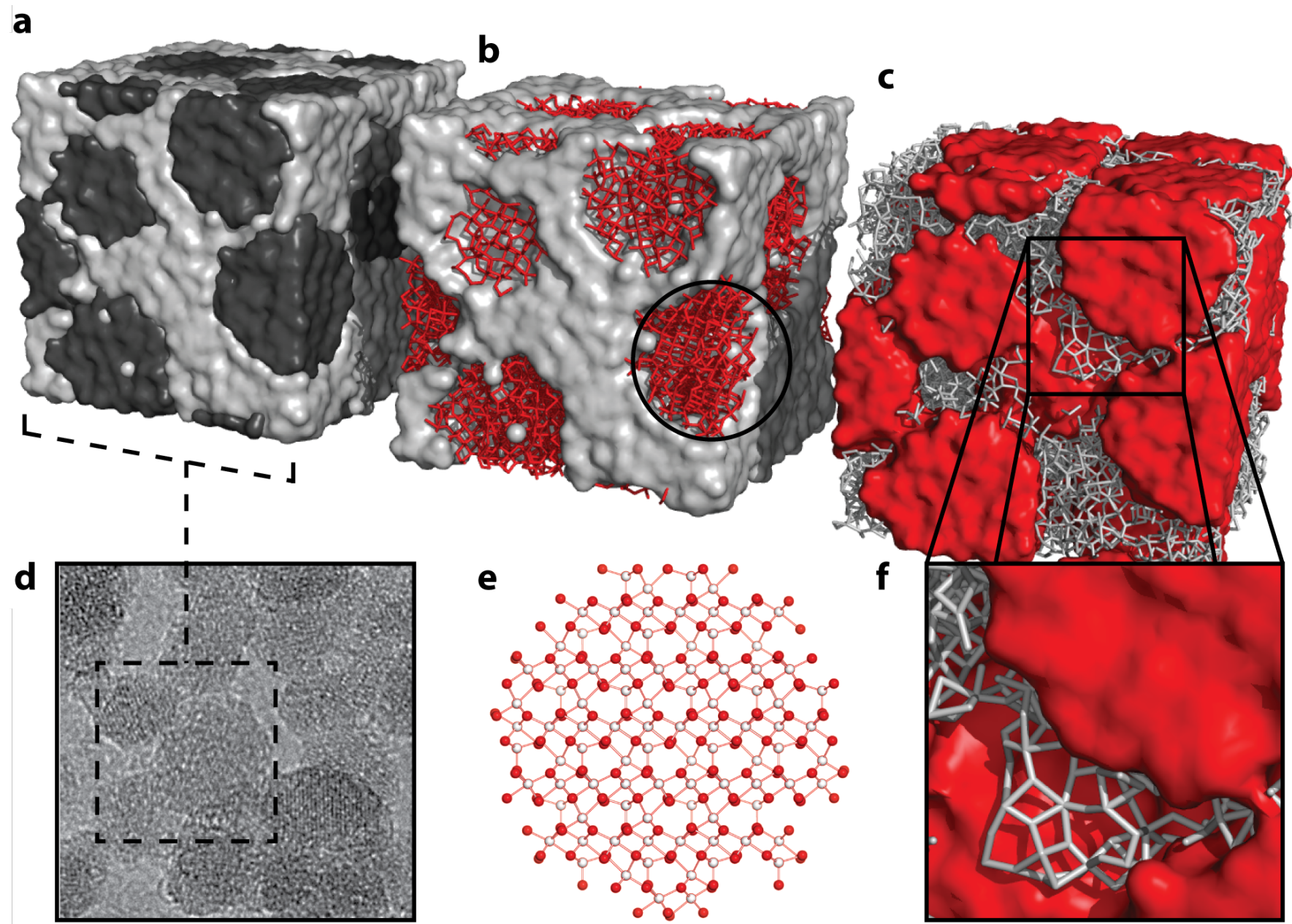


RMCProfile





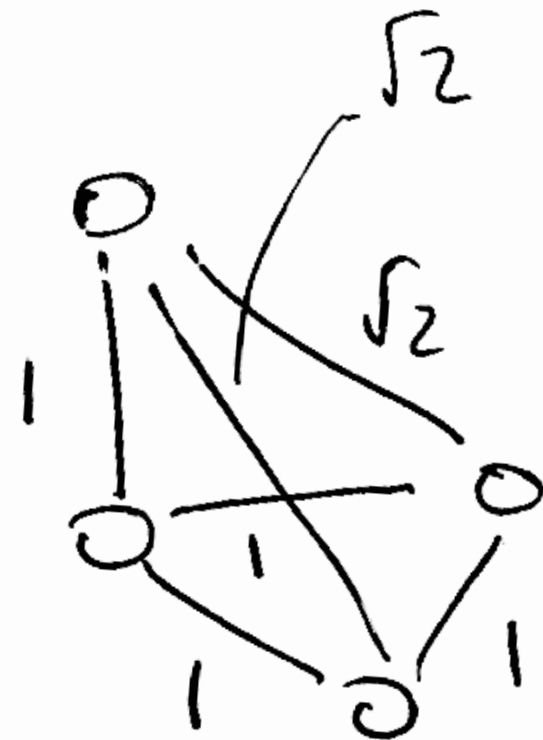
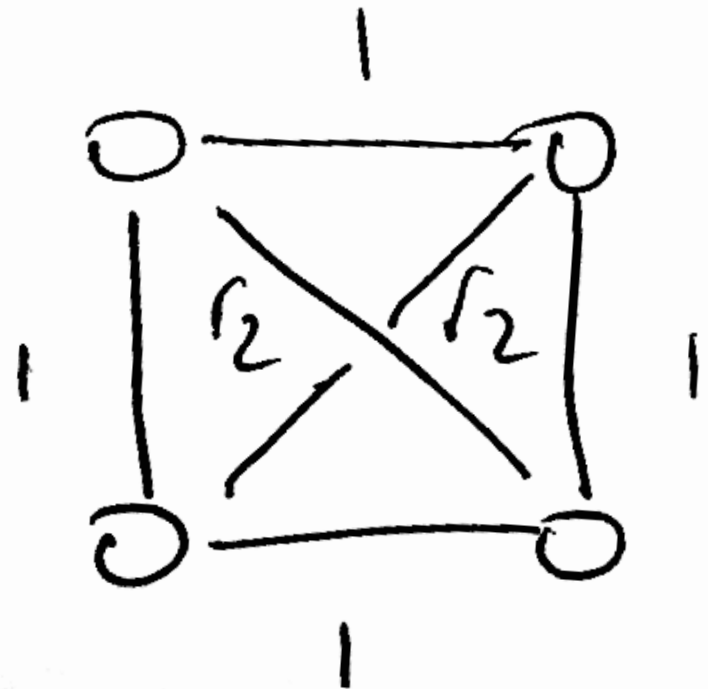




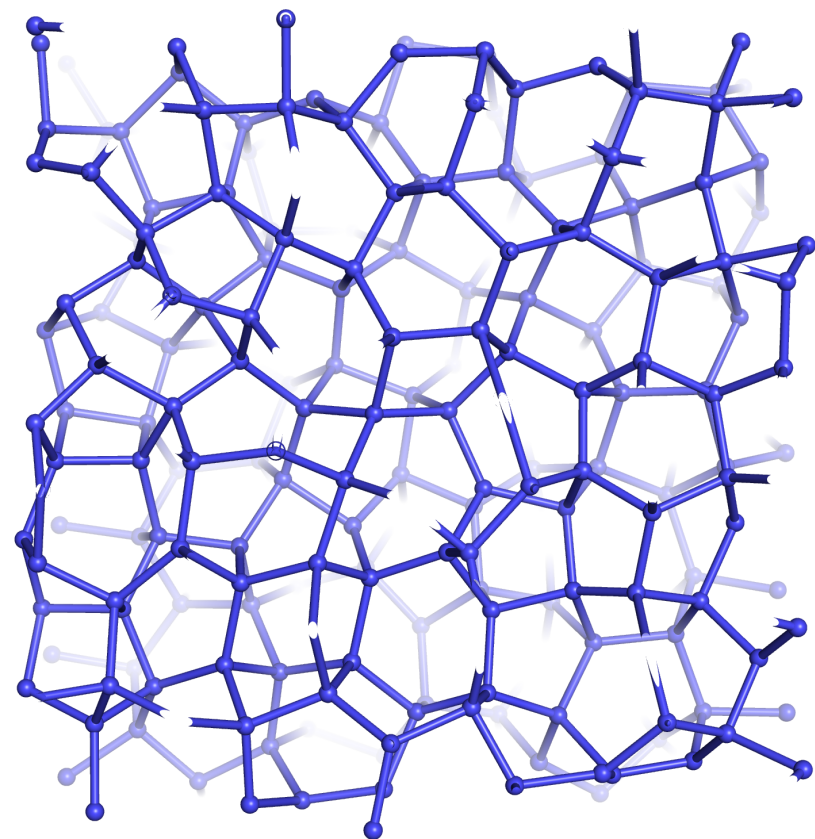
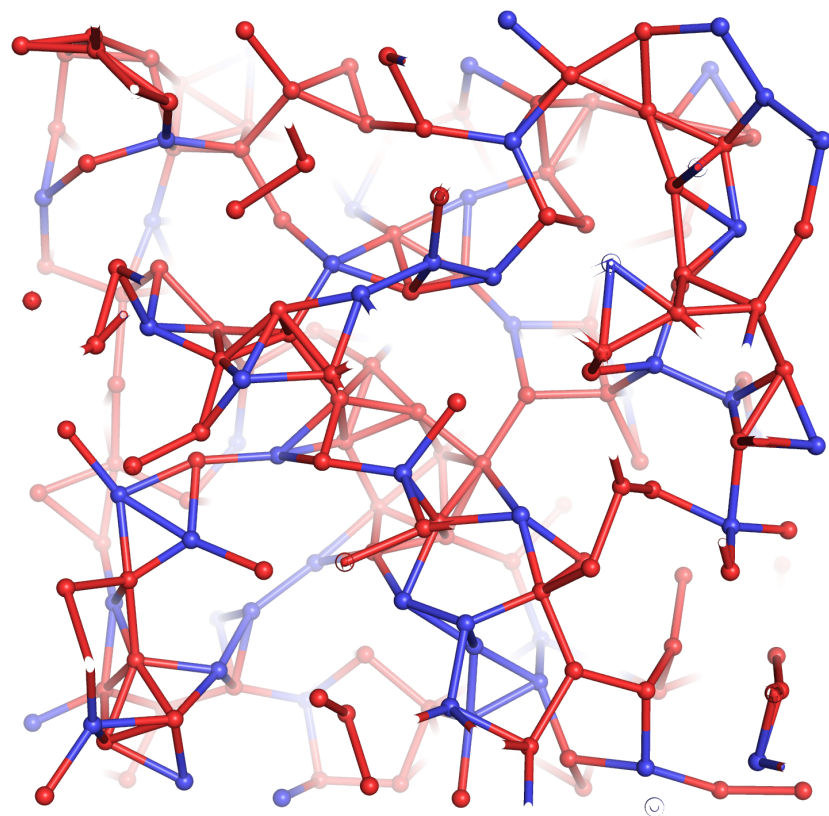
RMC: pros and cons

- + Arbitrary degrees/types of disorder
- + Simultaneous fits to real and reciprocal space
- + Interface with MD

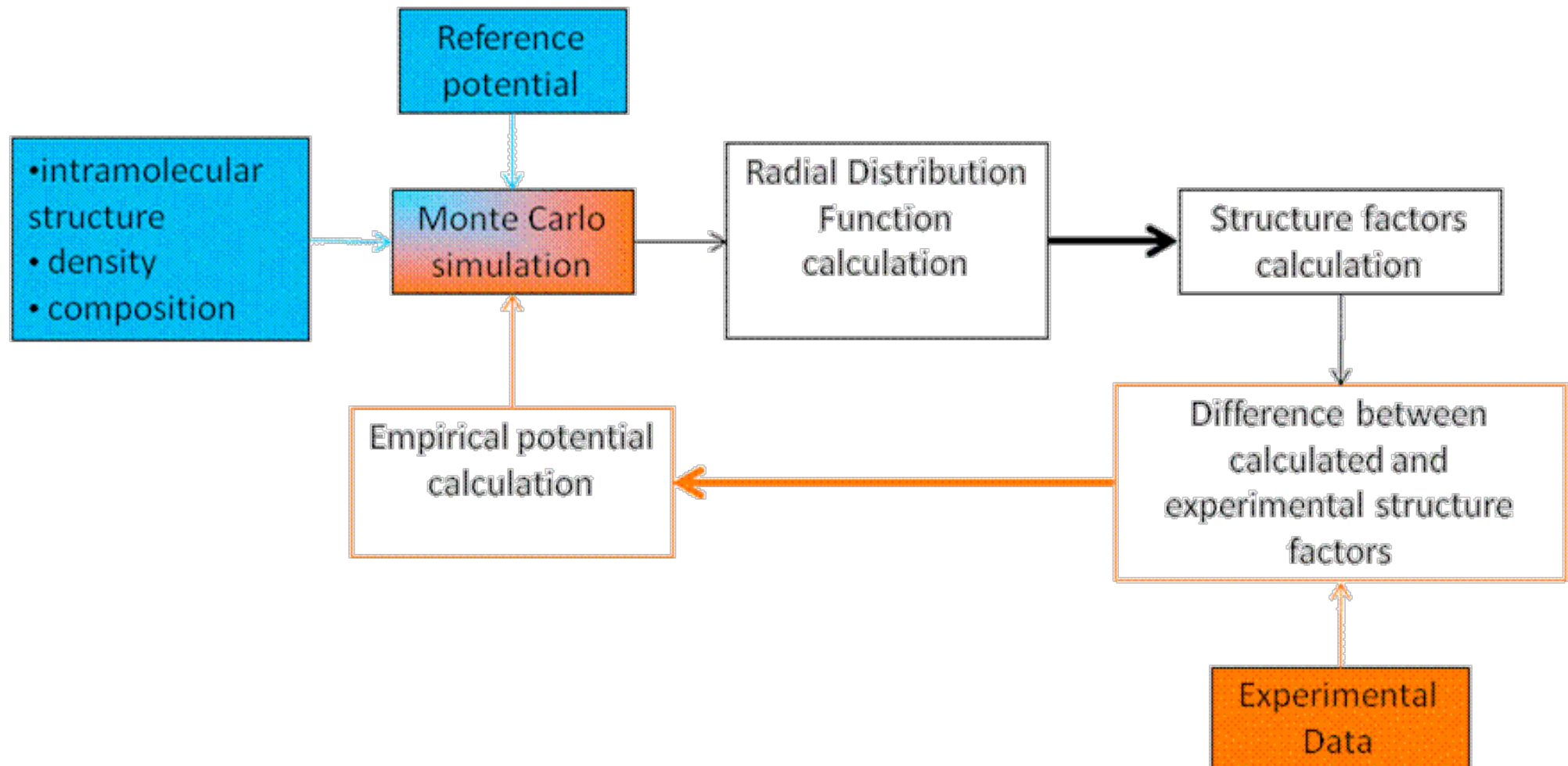
- Enormous entry barrier
- Resource (time/effort) intensive
- Model uniqueness / need for restraints



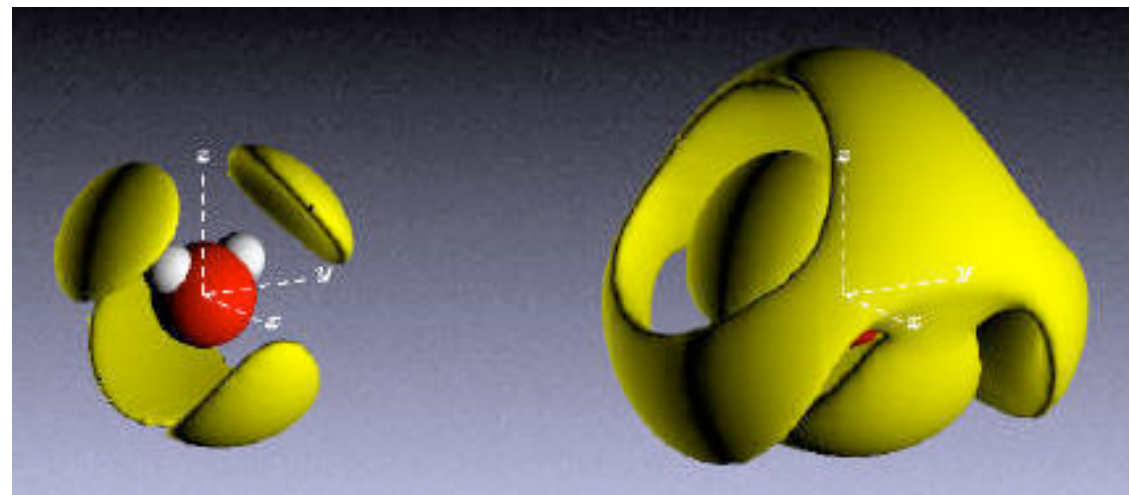
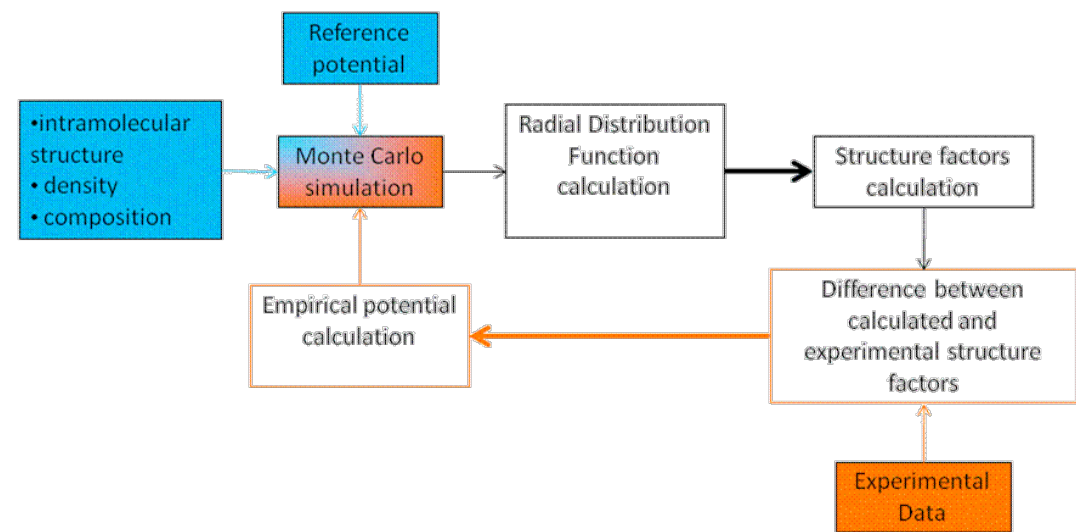
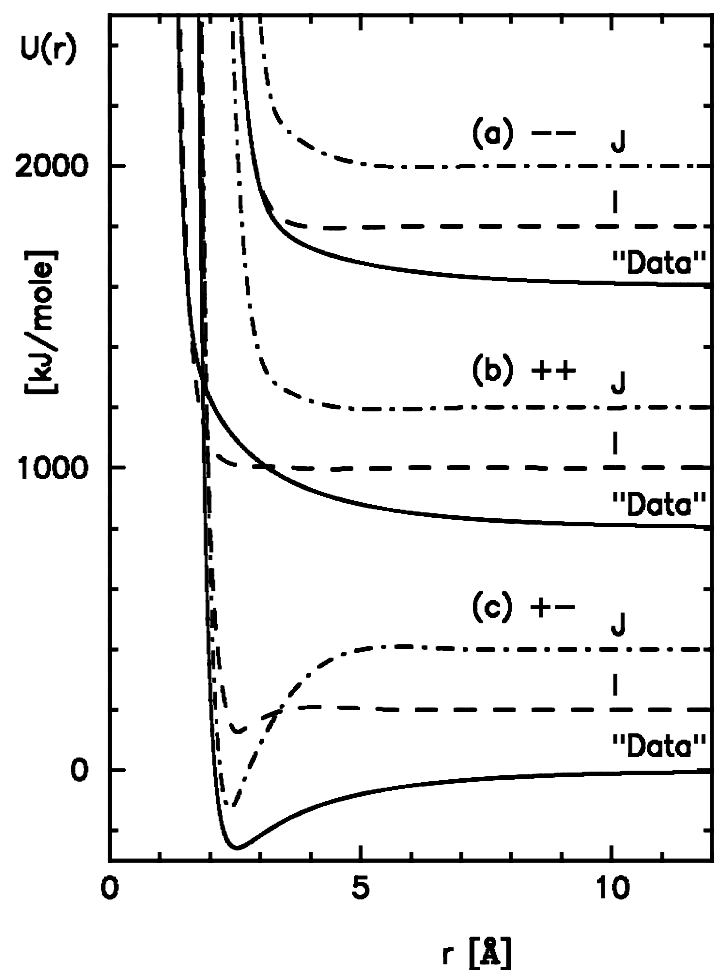
amorphous Si

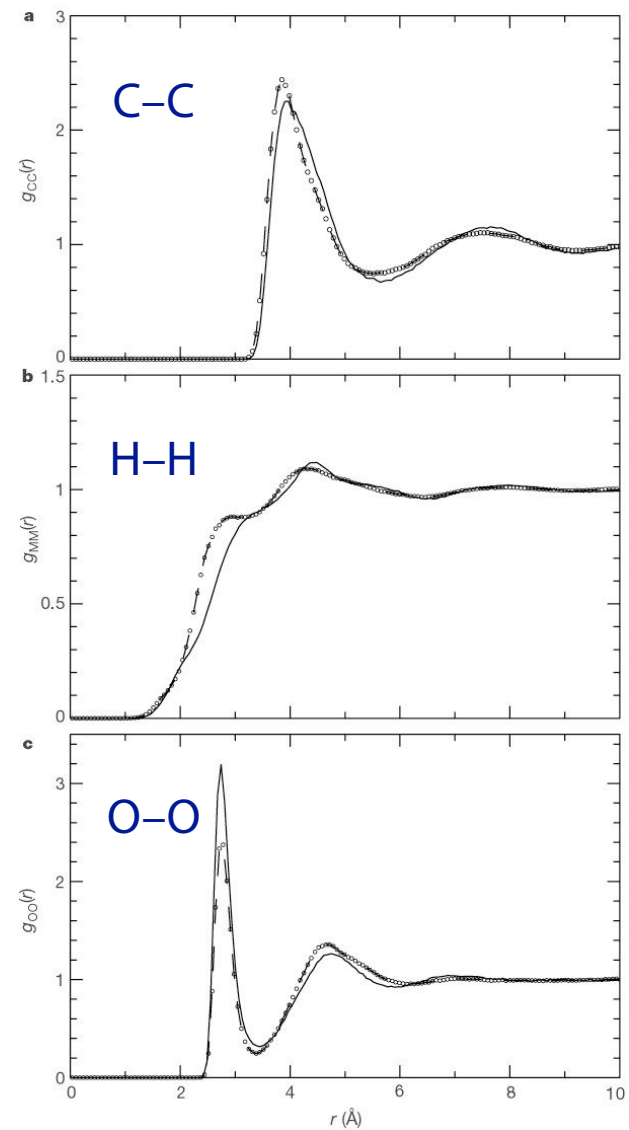
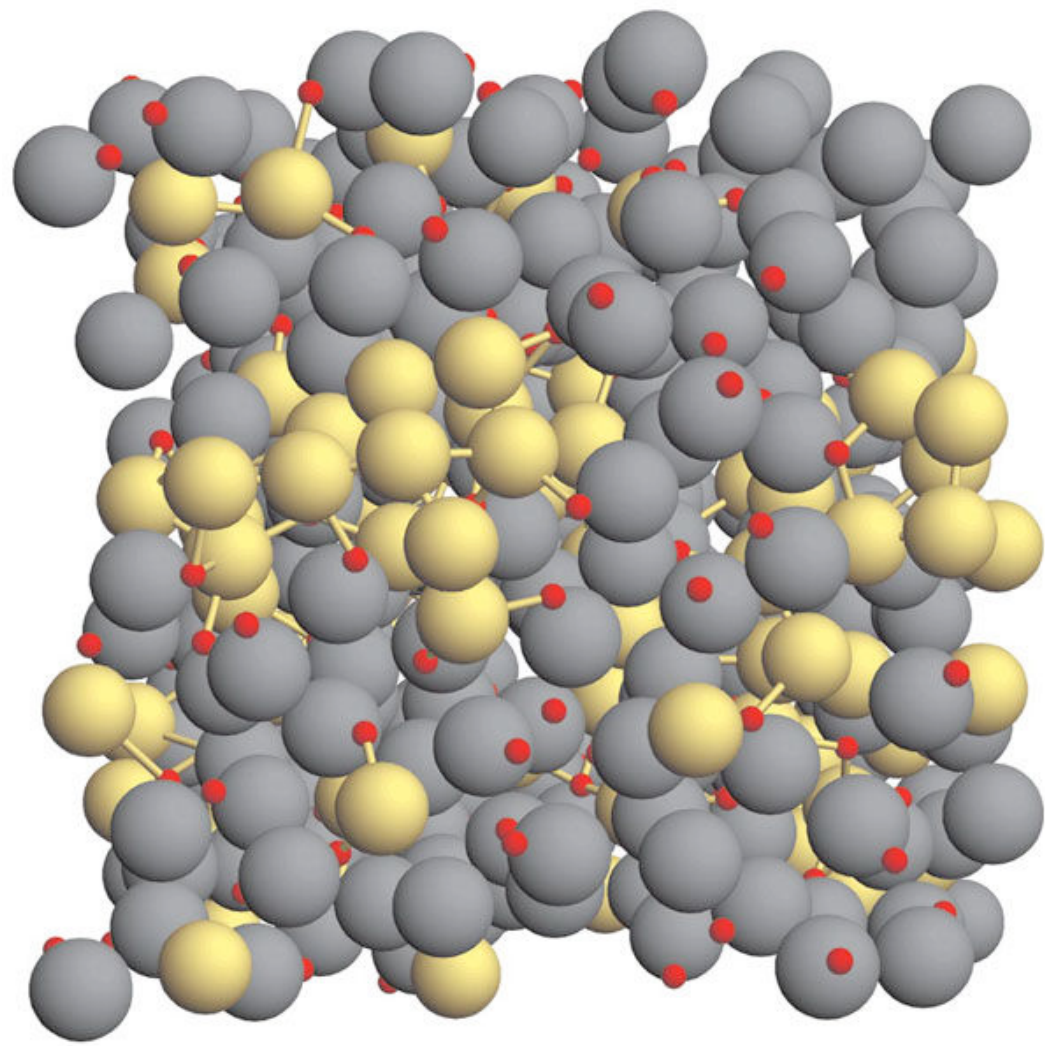


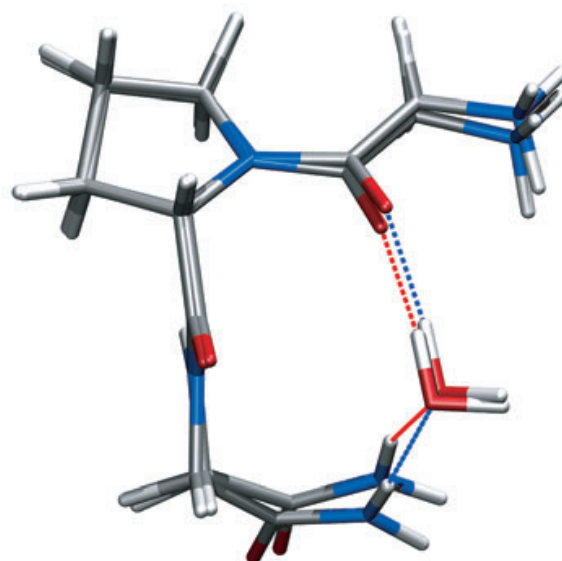
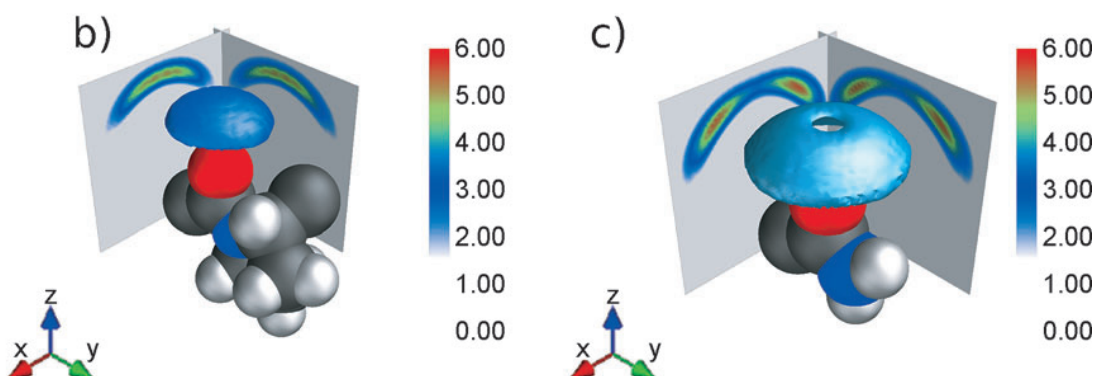
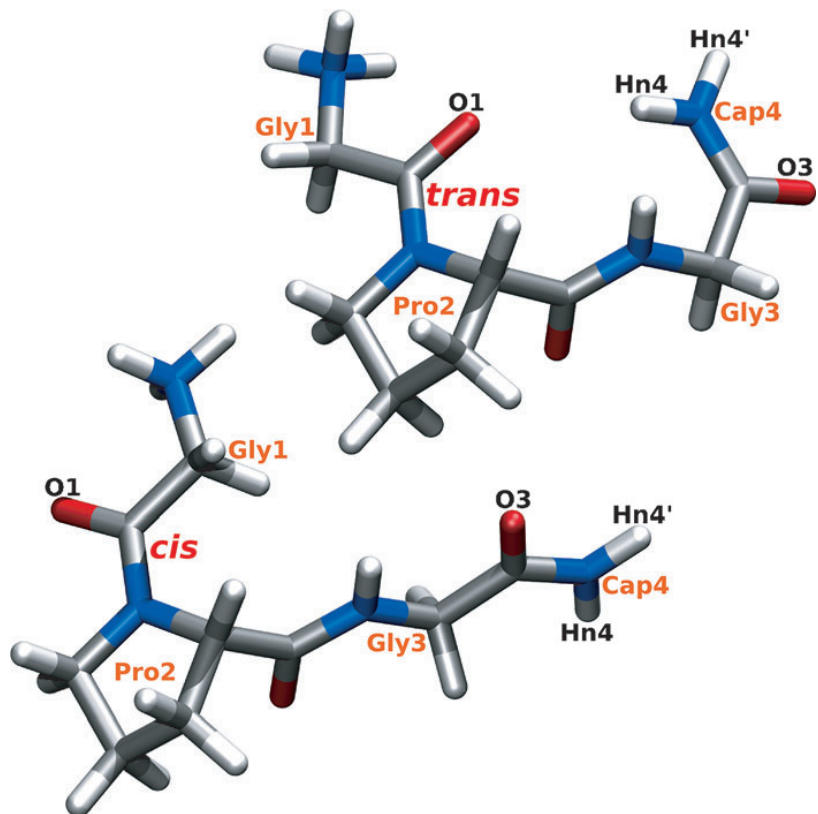
EPSR



EPSR



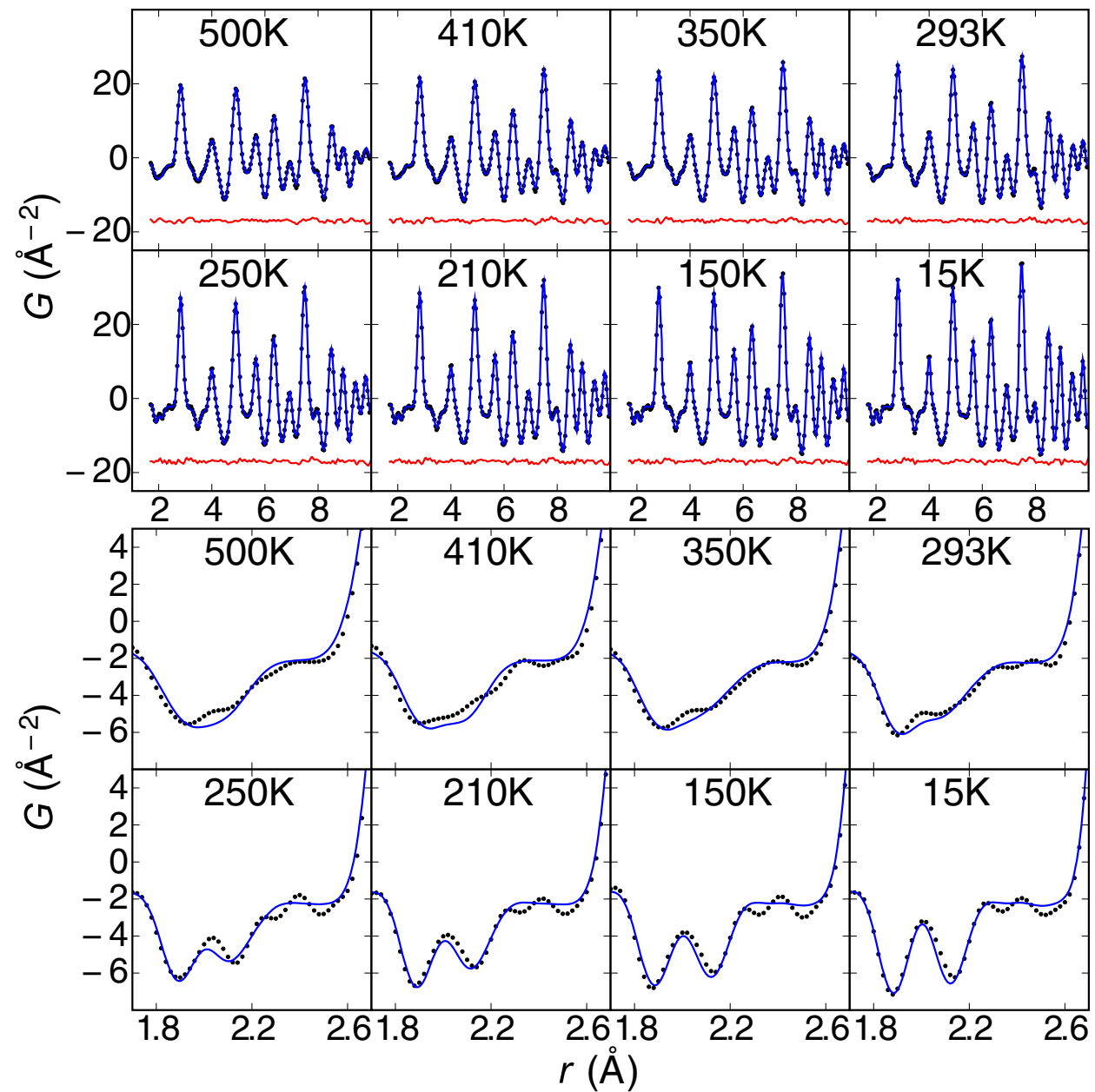
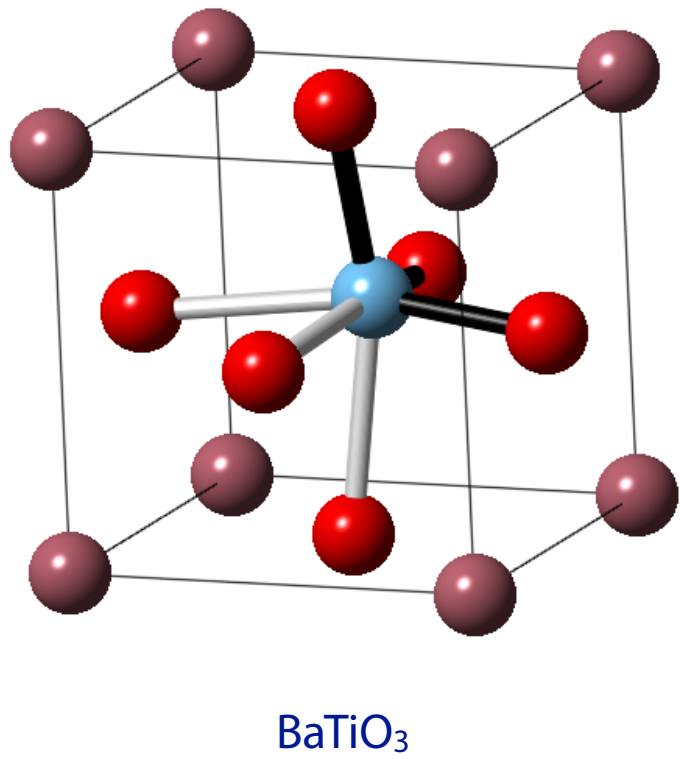




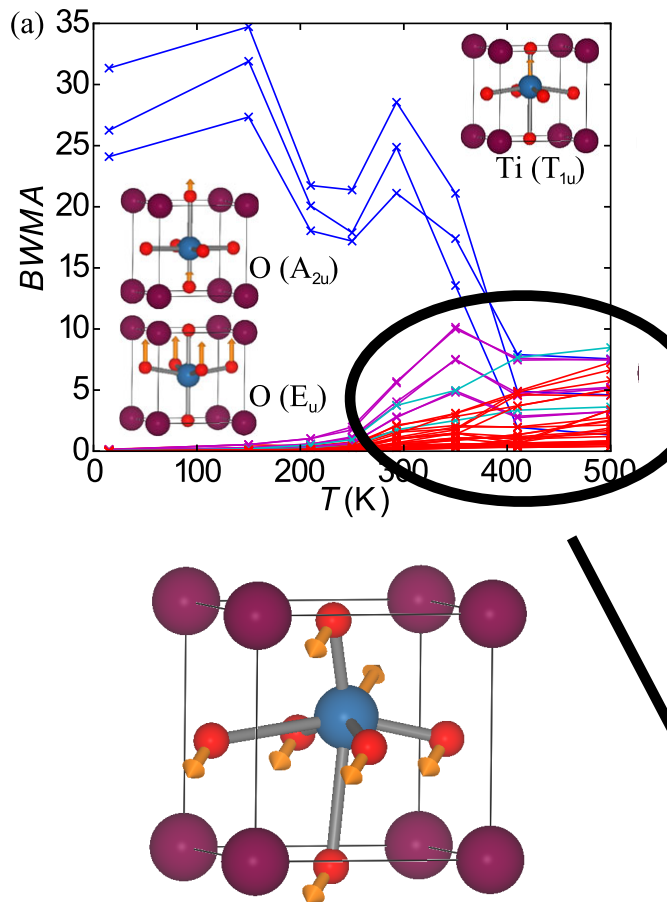
EPSR: pros and cons

- + Arbitrary degrees/types of disorder
- + Potentials as output
- + Ideal for liquids / glasses

- Need appropriate potentials
- Resource (time/effort) intensive
- Model uniqueness

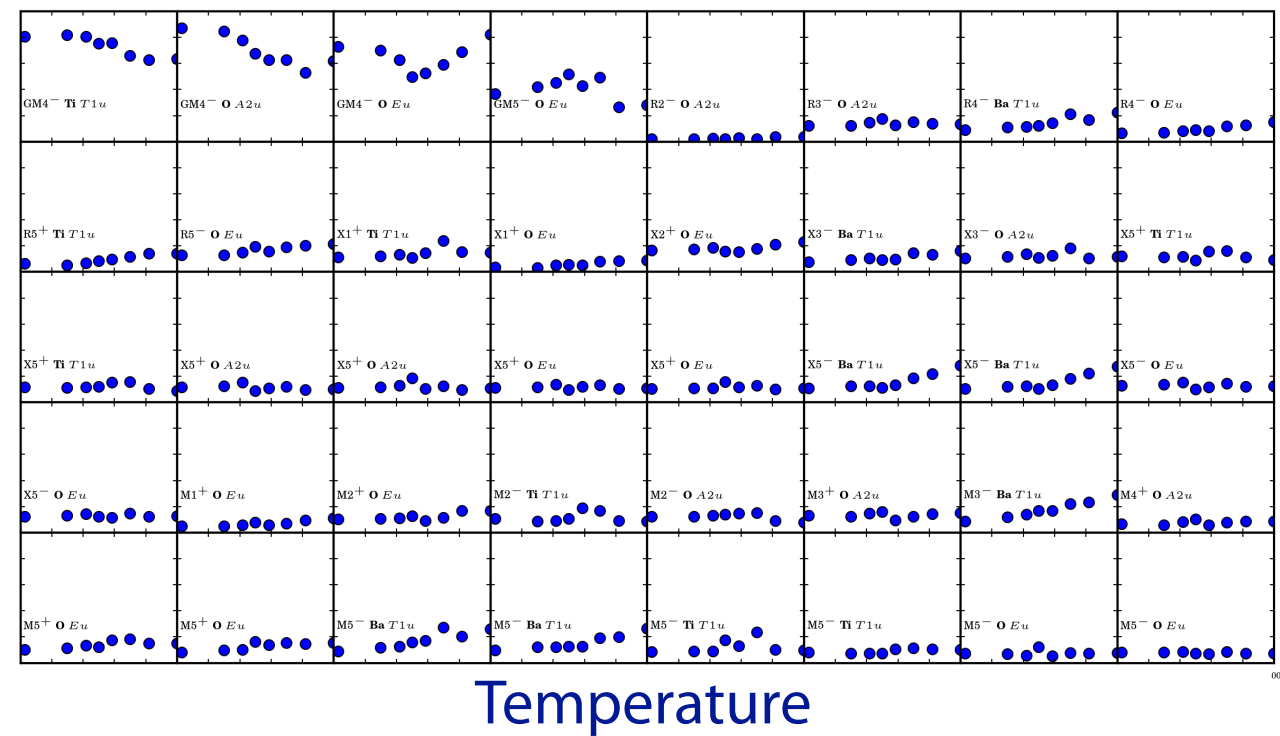


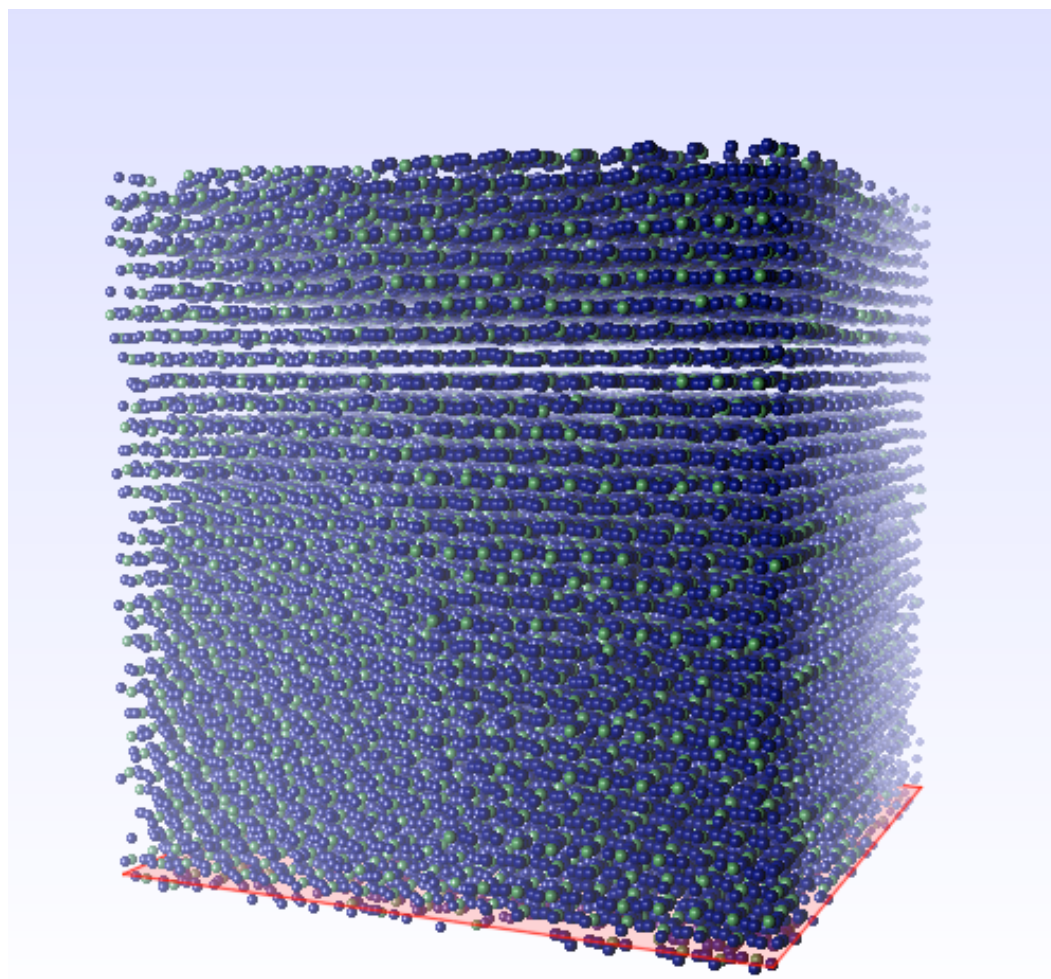
Local distortion modes

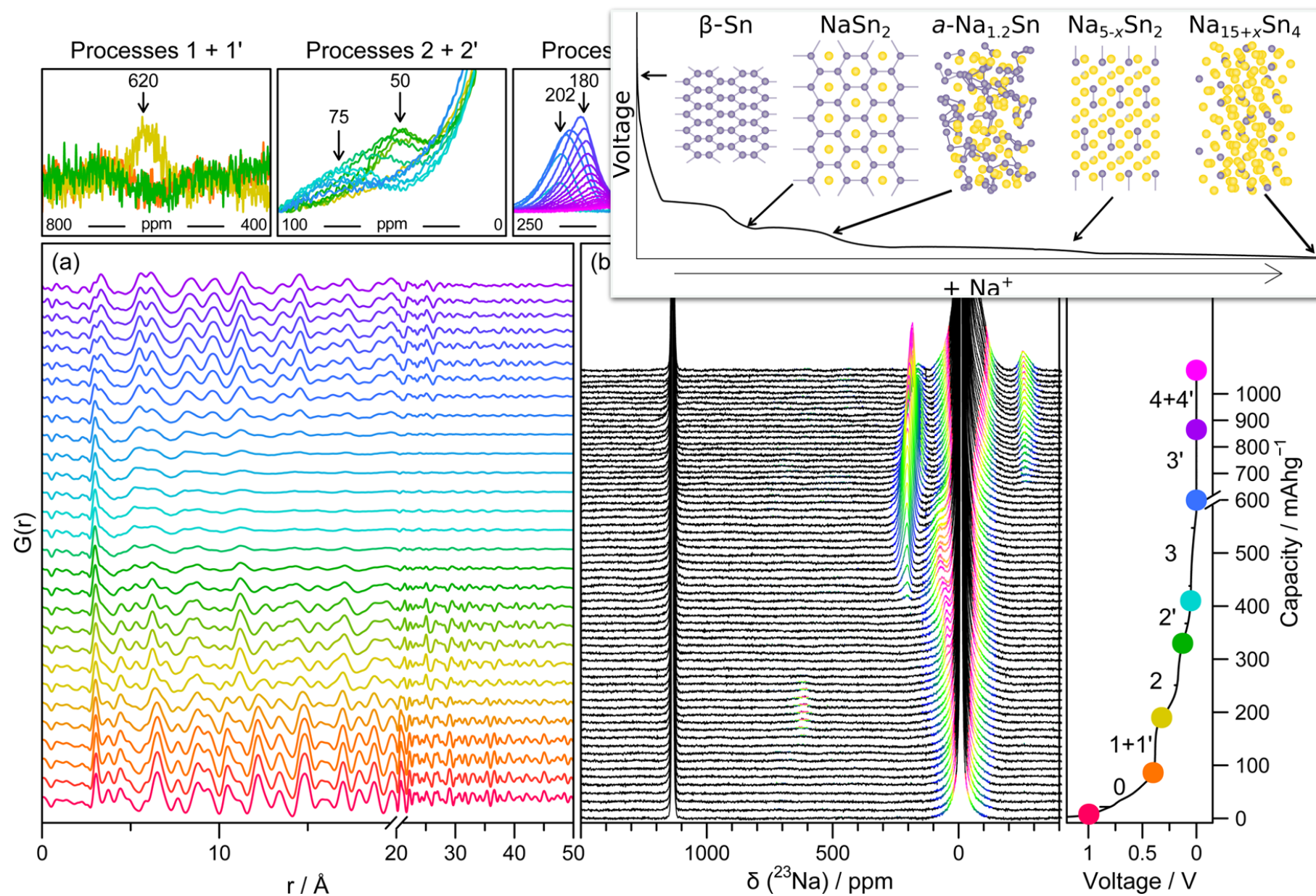


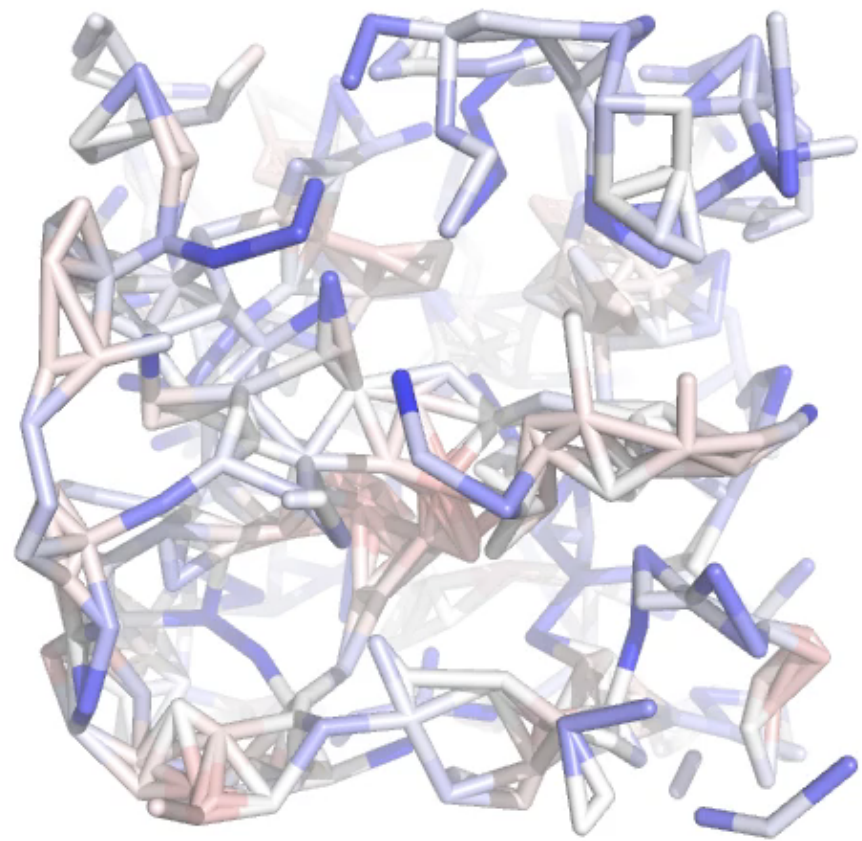
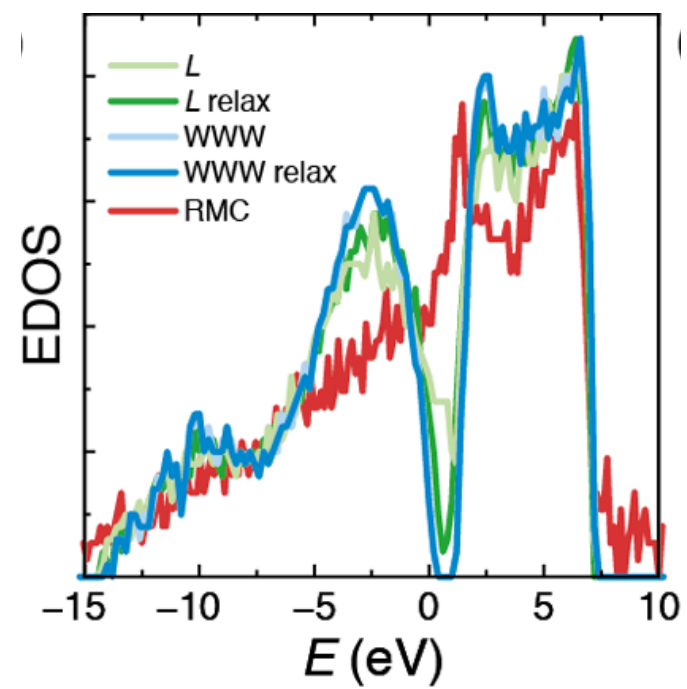
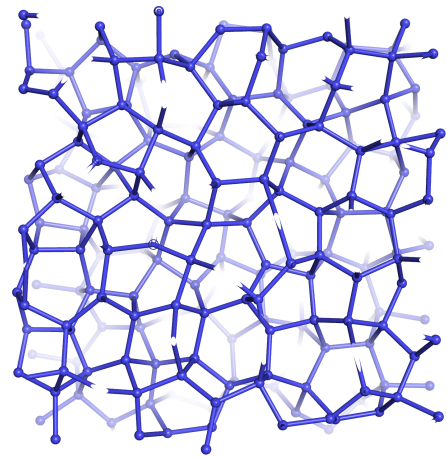
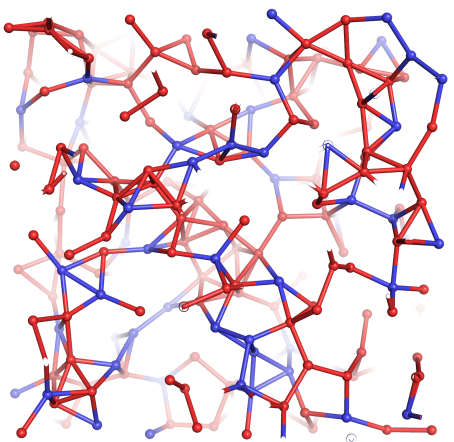
Importance of mode in fitting
PDF data

Same distortion;
different k









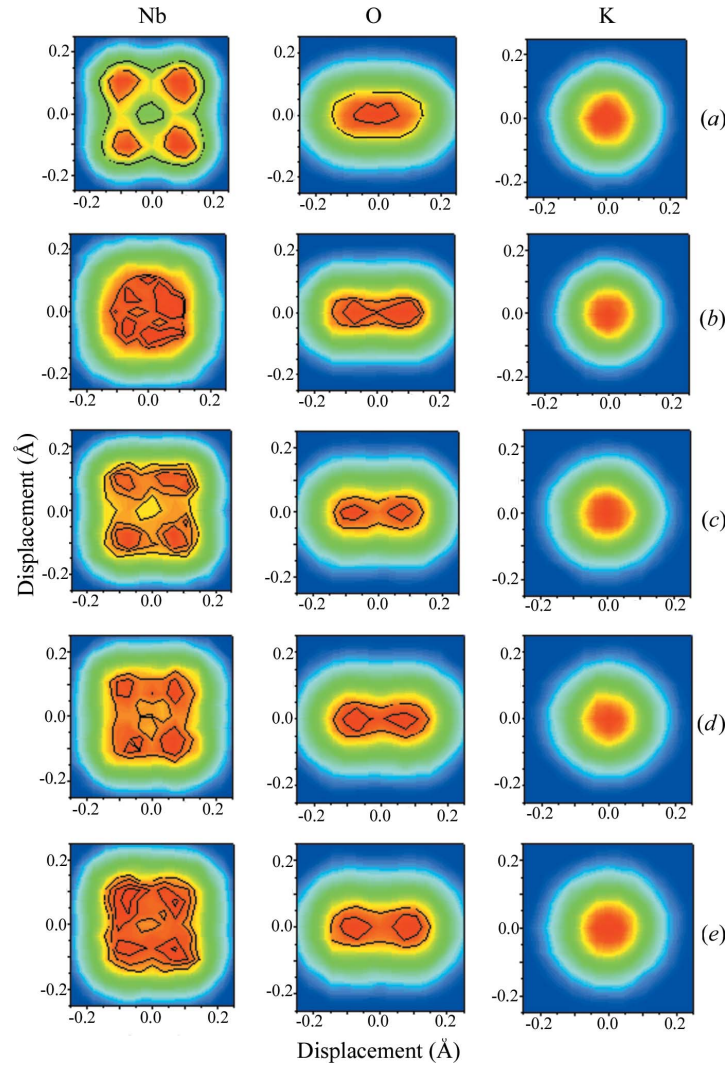


Figure 3

Probability density distributions for Nb, O and K projected onto the $\{100\}$ plane for the simulated structure (a) and for models obtained by fitting $G(r)$ (b), $G(r) + \text{Bragg}$ (c), $G(r) + \text{Bragg} + \text{EXAFS}$ (d) and $G(r) + \text{Bragg} + \text{EXAFS} + \text{electron diffuse scattering}$ (e). The images represent the sums of projections onto the three inequivalent $\{100\}$ planes.

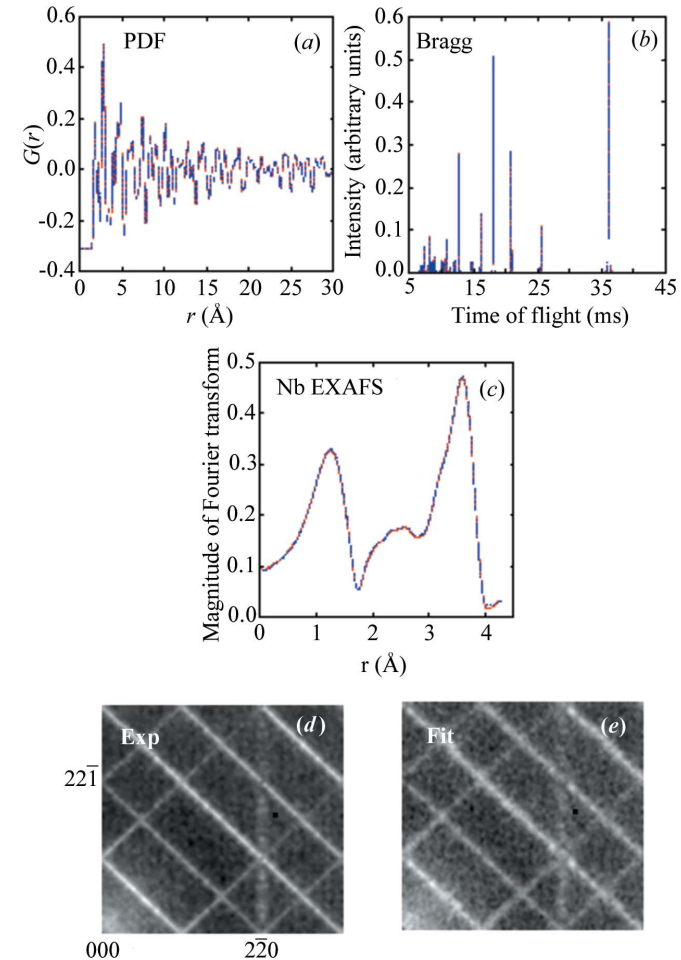
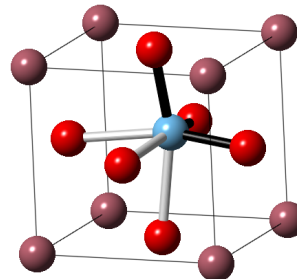
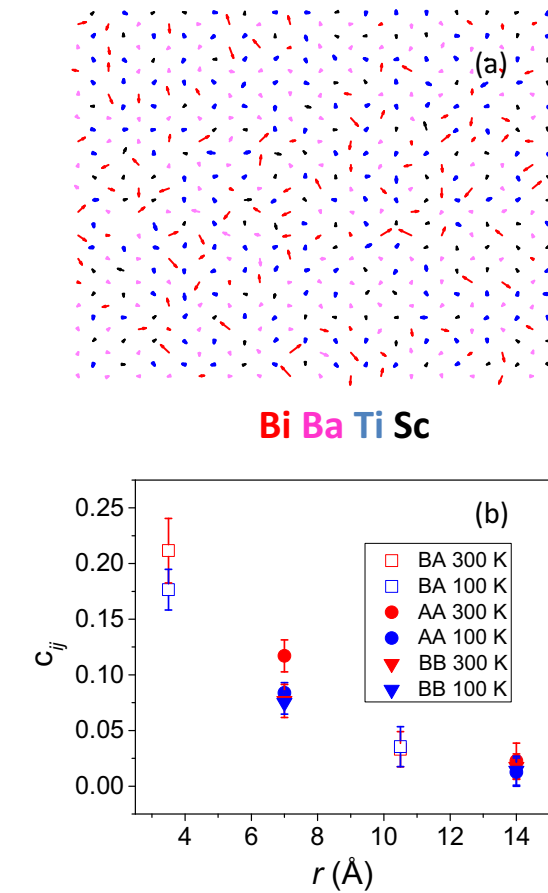
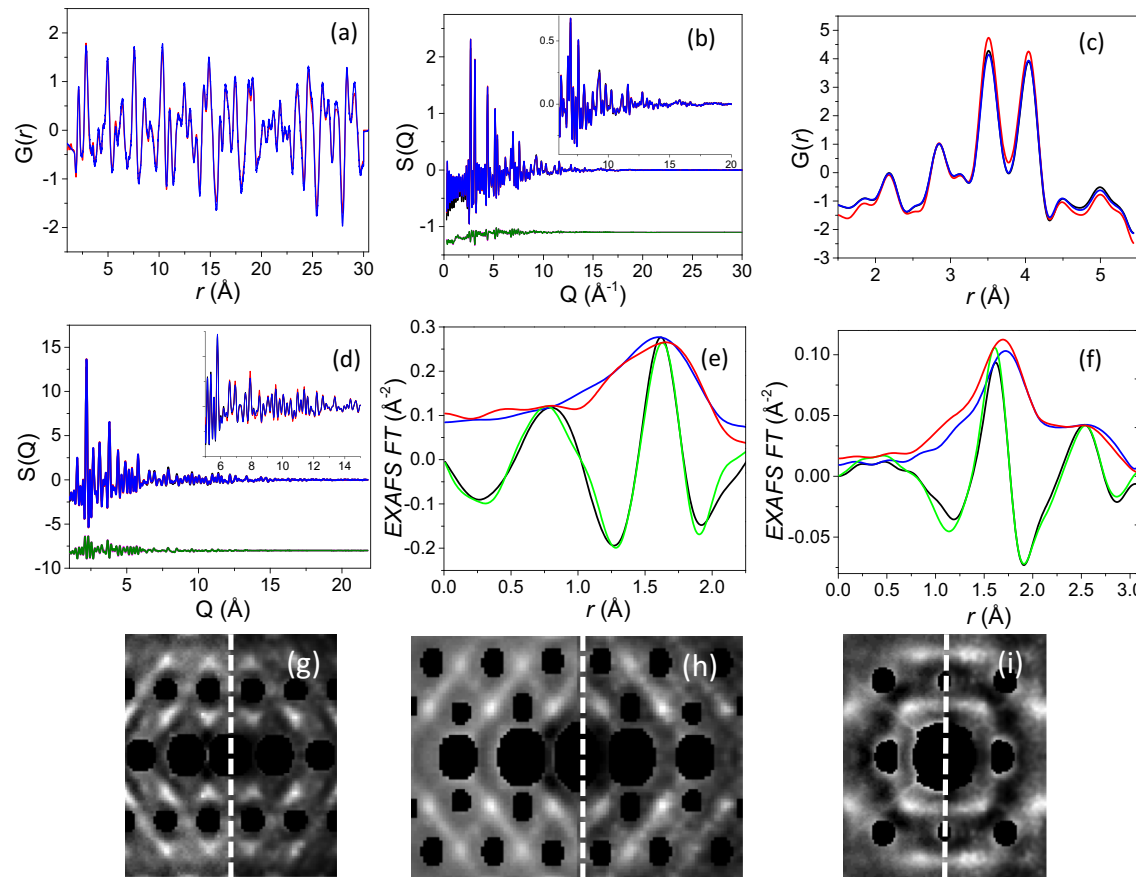


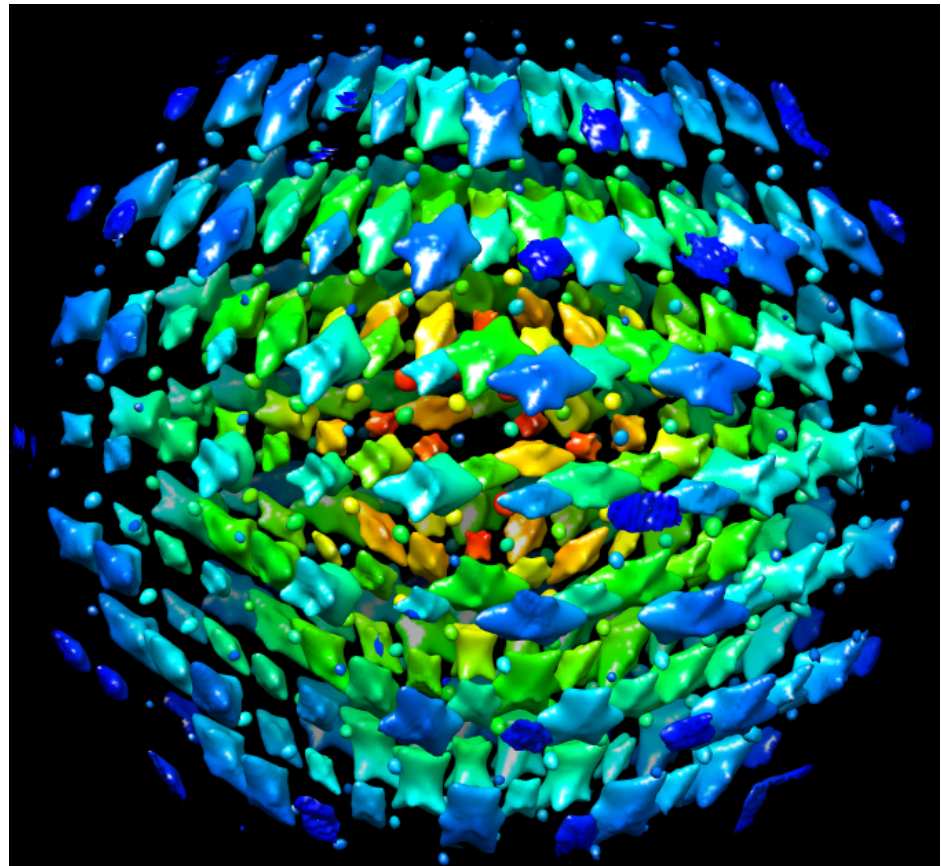
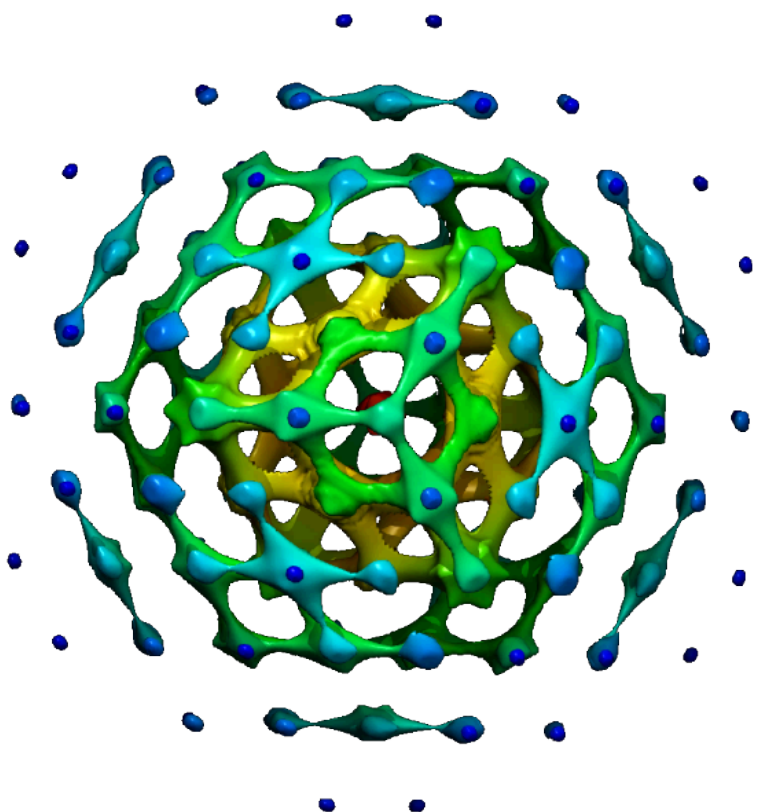
Figure 4

Simulated ('experimental') and fitted neutron $G(r)$ (a), neutron Bragg profile (b), magnitude of the Nb EXAFS Fourier transform (c) and electron diffuse scattering in the $\{114\}$ reciprocal-lattice section (d). The locations of Bragg reflections in the electron diffraction pattern are indicated. The 'experimental' and fitted data are indicated using dotted red and solid blue lines, respectively. The fitted data correspond to a model obtained using simultaneous fitting of all the data sets (*i.e.* Fit 4; for details see text). The quality of fit is so good that the experimental and calculated traces overlap completely. The fitted electron diffuse scattering is shown in (e).

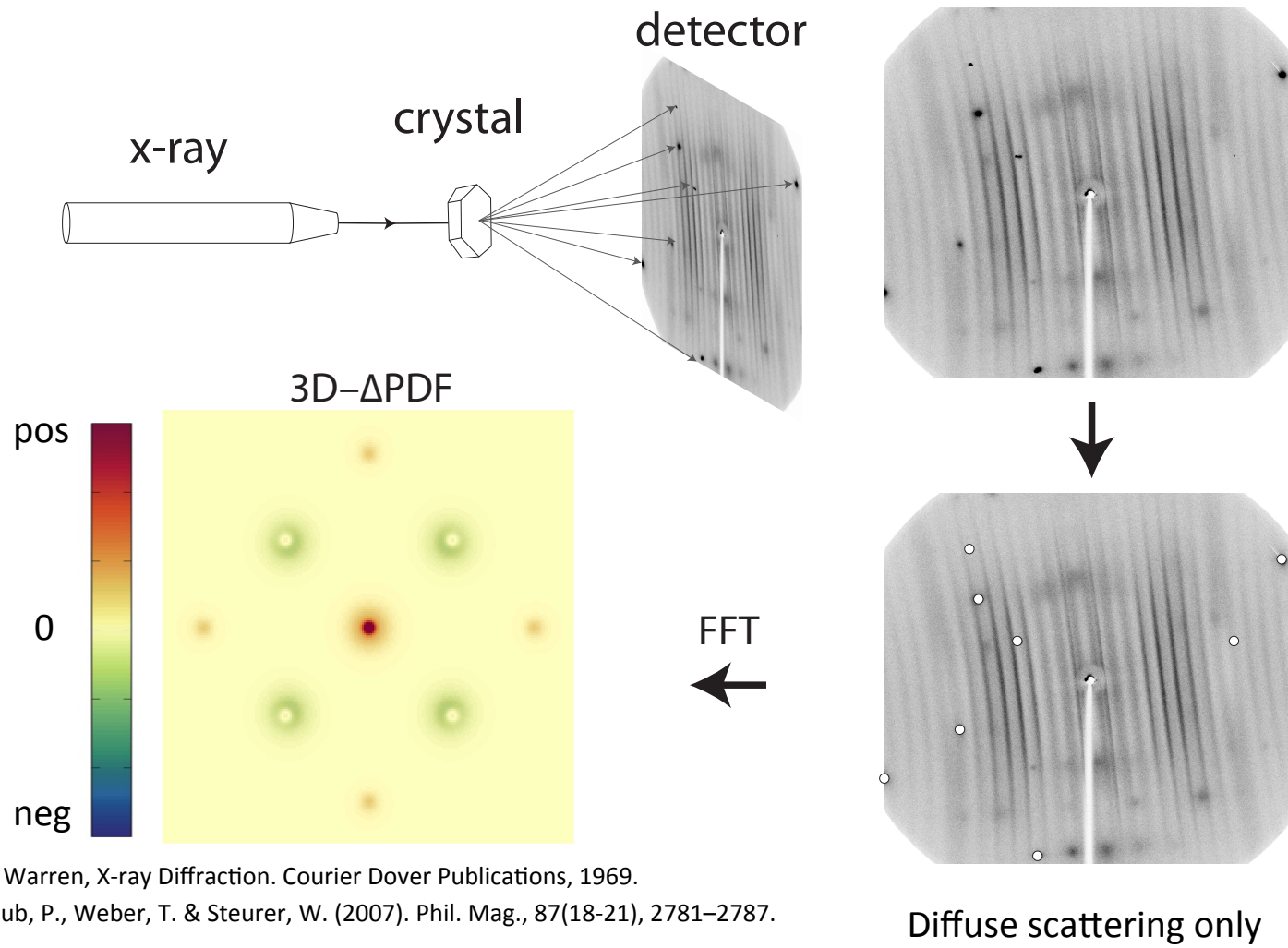
Local structure in $\text{BaTiO}_3\text{-BiScO}_3$ dipole glasses

I. Levin,^{1,*} V. Krayzman,¹ J. C. Woicik,¹ F. Bridges,² G. E. Sterbinsky,³ T-M. Usher,⁴ J. L. Jones,⁴ and D. Torrejon⁵



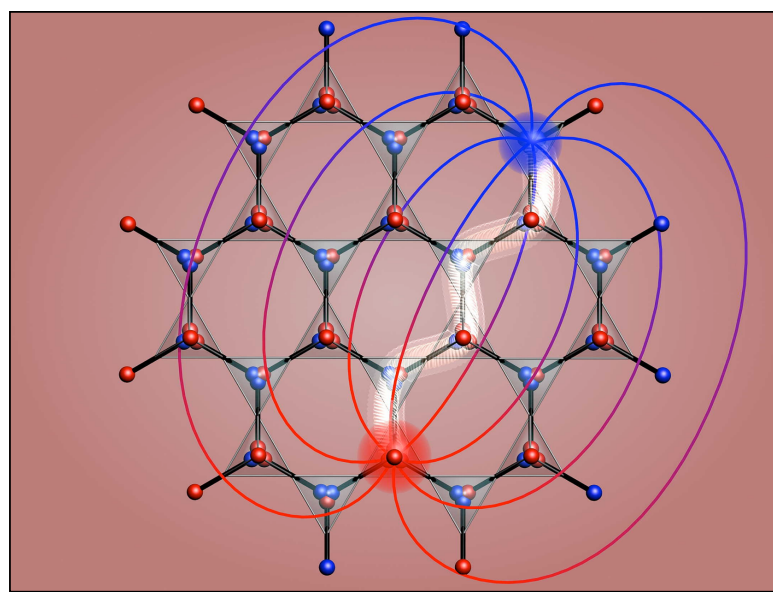
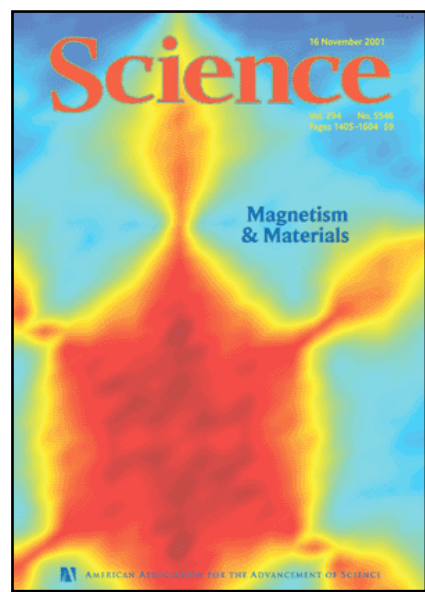
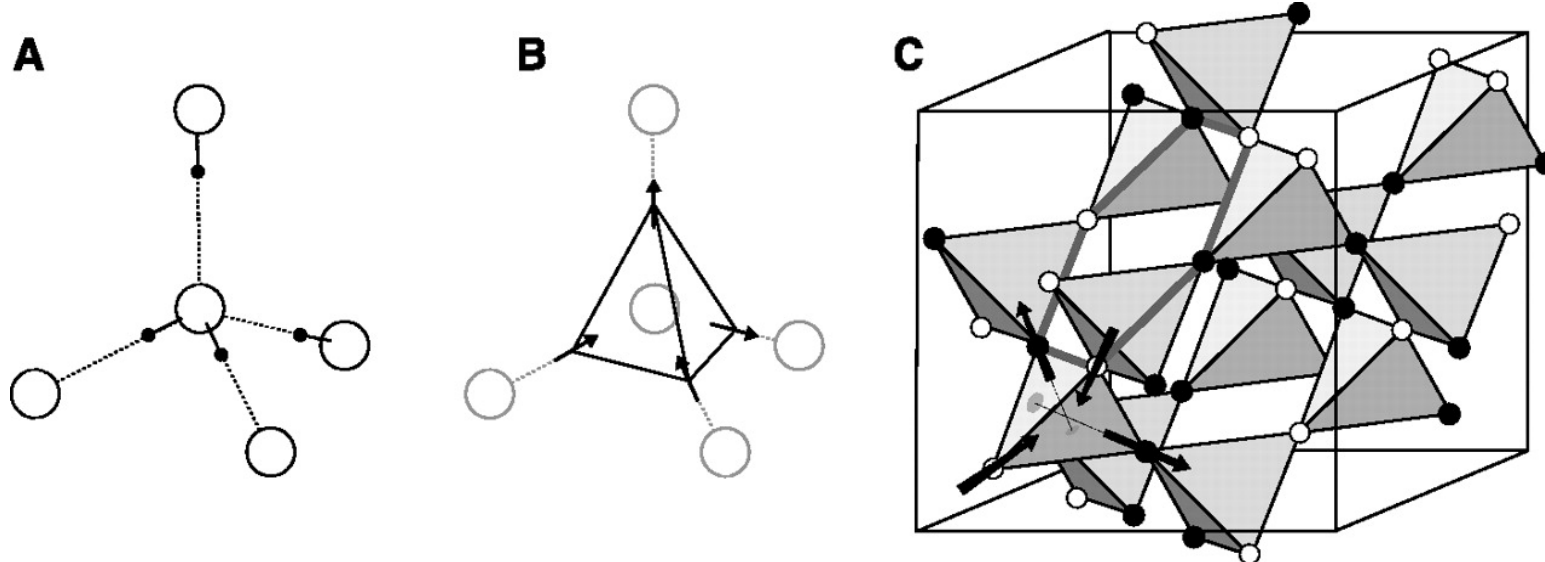


Three dimensional difference pair distribution function (3D- Δ PDF)

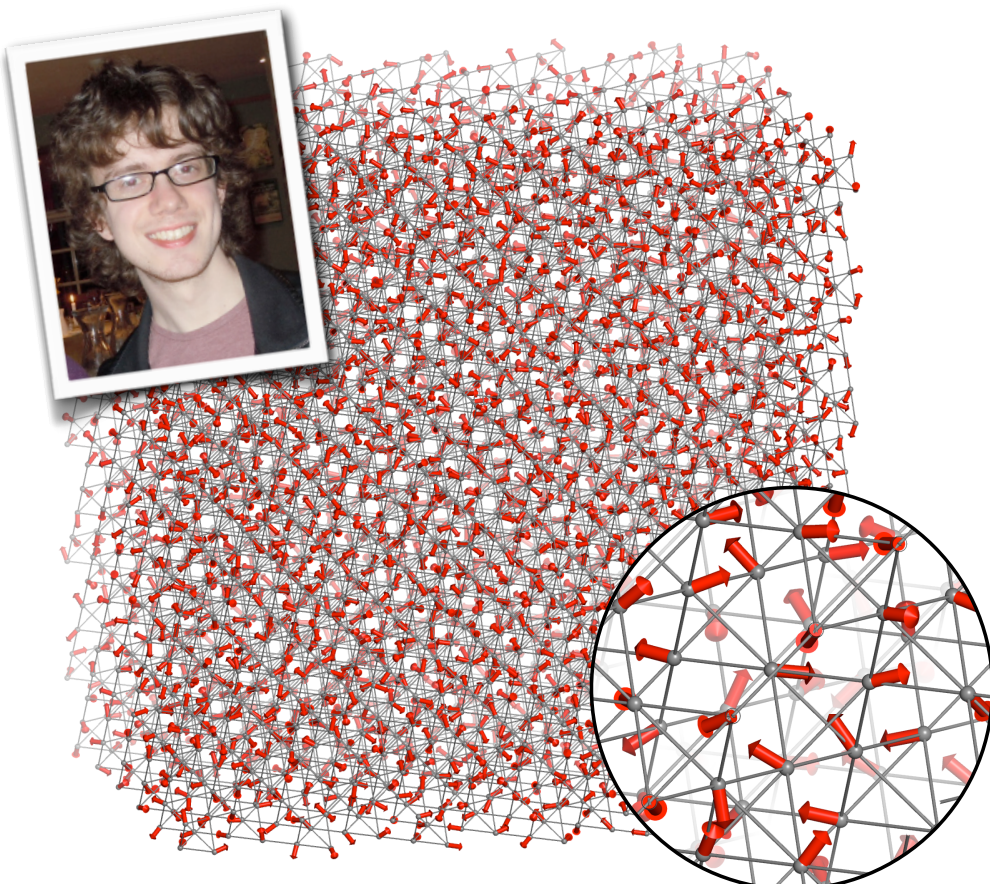


B. E. Warren, X-ray Diffraction. Courier Dover Publications, 1969.

Schaub, P., Weber, T. & Steurer, W. (2007). Phil. Mag., 87(18-21), 2781–2787.



Spinvert – static atom approximation



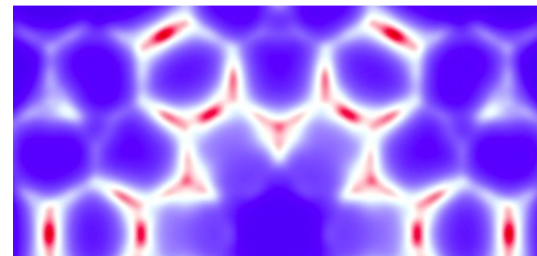
$$I(\mathbf{Q}) = \frac{1}{N} \left| \sum_i \mathbf{S}_{\perp i} p_i(Q) \exp(i\mathbf{Q} \cdot \mathbf{r}_i) \right|^2$$

$$I(Q) = p(Q)^2 \left\{ \frac{2}{3} + \int r^2 \left[A(r) \frac{\sin Qr}{Qr} + B(r) \left(\frac{\sin Qr}{(Qr)^3} - \frac{\cos Qr}{(Qr)^2} \right) \right] dr \right\}$$

spinvert.chem.ox.ac.uk

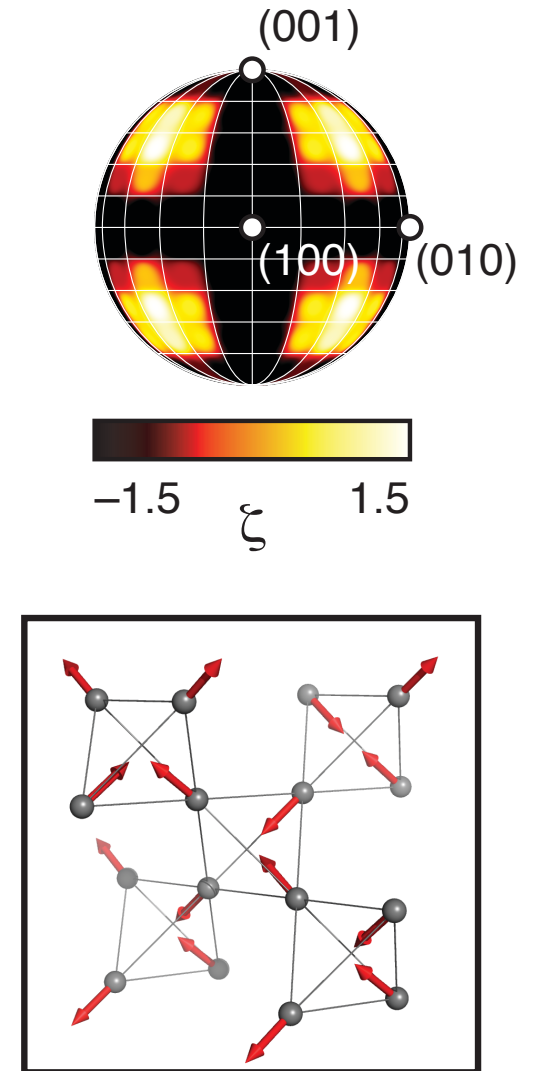
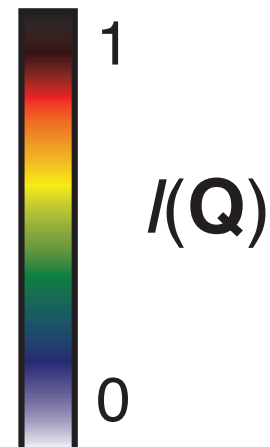
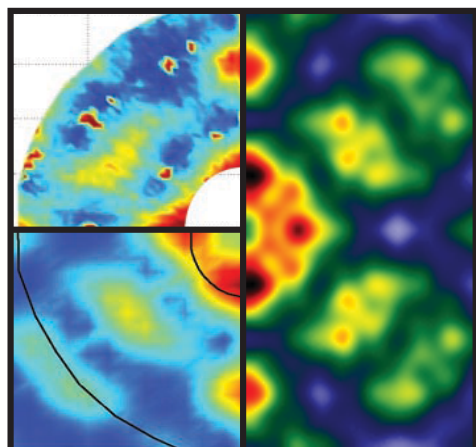
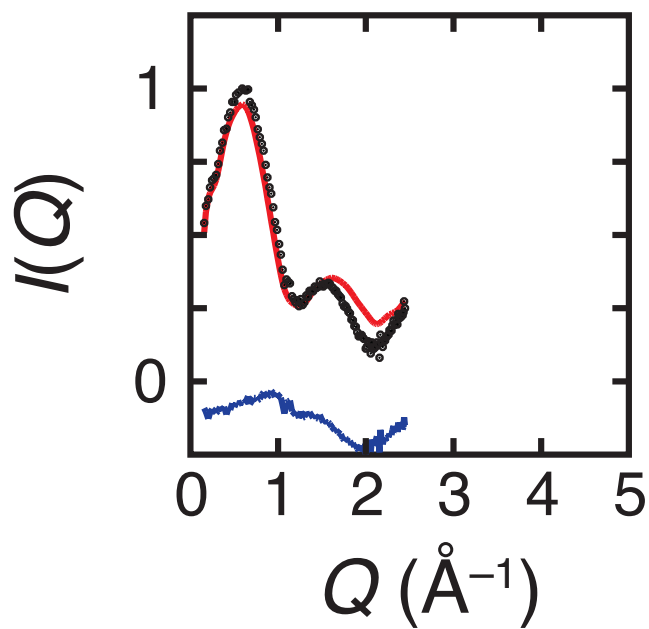
Spinvert

Magnetic structure refinement for paramagnets



[Click here to download program, instructions and examples](#)

Spin ice — $\text{Ho}_2\text{Ti}_2\text{O}_7$



Total scattering: future directions

- * Small angle scattering / multiple lengthscales
- * Dynamics
- * Interface with computation (esp. *ab initio*)
- * Complex sample environments (p , E , B)
- * Thin film
- * Heterostructures / spatial resolution
- * 3D
- * Analysis – robustness / ease